This is an electronic reprint of the original article.
This reprint *may differ* from the original in pagination and typographic detail.

Author(s): Katja T. Rinne-Garmston, Gerhard Helle, Marco M. Lehmann, Elina Sahlstedt, Jürgen Schleucher & John S. Waterhouse

Title: Newer Developments in Tree-Ring Stable Isotope Methods

Year: 2022

Version: Published version

Copyright: The Author(s) 2022

Rights: CC BY 4.0

Rights url: http://creativecommons.org/licenses/by/4.0/

Please cite the original version:

Rinne-Garmston, K.T., Helle, G., Lehmann, M.M., Sahlstedt, E., Schleucher, J., Waterhouse, J.S. (2022). Newer Developments in Tree-Ring Stable Isotope Methods. In: Siegwolf, R.T.W., Brooks, J.R., Roden, J., Saurer, M. (eds) Stable Isotopes in Tree Rings. Tree Physiology, vol 8. Springer, Cham. https://doi.org/10.1007/978-3-030-92698-4_7.

Chapter 7
Newer Developments in Tree-Ring Stable Isotope Methods

Check for updates

Katja T. Rinne-Garmston, Gerhard Helle, Marco M. Lehmann, Elina Sahlstedt, Jürgen Schleucher, and John S. Waterhouse

Abstract The tree-ring stable C, O and H isotope compositions have proven valuable for examining past changes in the environment and predicting forest responses to environmental change. However, we have not yet recovered the full potential of this archive, partly due to a lack understanding of fractionation processes resulting from methodological constraints. With better understanding of the biochemical and tree physiological processes that lead to differences between the isotopic compositions of primary photosynthates and the isotopic compositions of substrates deposited in stem xylem, more reliable and accurate reconstructions could be obtained. Furthermore, by extending isotopic analysis of tree-ring cellulose to intra-molecular level, more information could be obtained on changing climate, tree metabolism or ecophysiology. This chapter presents newer methods in isotope research that have become available or show high future potential for fully utilising the wealth of information available in tree-rings. These include compound-specific analysis of sugars and cyclitols, high spatial resolution analysis of tree rings with UV-laser, and position-specific isotope analysis of cellulose. The aim is to provide the reader with understanding of

K. T. Rinne-Garmston (✉) · E. Sahlstedt
Natural Resources Institute Finland (Luke), Latokartanonkaari 9, 00790 Helsinki, Finland
e-mail: katja.rinne-garmston@luke.fi

E. Sahlstedt
e-mail: elina.sahlstedt@luke.fi

G. Helle
Helmholtz-Centre Potsdam, GFZ German Centre for GeoSciences Section 4.3 Climate Dynamics and Landscape Evolution, Potsdam, Germany
e-mail: gerhard.helle@gfz-potsdam.de

M. M. Lehmann
Swiss Federal Institute for Forest, Snow and Landscape Research WSL, Birmensdorf, Switzerland
e-mail: marco.lehmann@alumni.ethz.ch

J. Schleucher
Department of Medical Biochemistry and Biophysics, Umeå University, 90187 Umeå, Sweden
e-mail: jurgen.schleucher@umu.se

J. S. Waterhouse
School of Life Sciences, Anglia Ruskin University, East Road, Cambridge CB1 1PT, UK
e-mail: john.waterhouse@aru.ac.uk

the advantages and of the current challenges connected with the use of these methods for stable isotope tree-ring research.

7.1   Introduction

Significant gaps still exist in our understanding about how a given isotopic composition of a tree ring is formed. This mainly concerns the metabolic processes and isotopic fractionations that occur post-photosynthetically in the leaf and phloem and also during tree-ring formation (see Chap. 13). To achieve a profound level of knowledge of these processes that impact the environmental signal extractable from tree-ring δ^2H, $\delta^{13}C$ and $\delta^{18}O$ values, it is necessary to go beyond the conventional analytical methods in isotope analysis, which utilize "bulk" matter (e.g. leaves or sugar extract) and to focus on studies at intra-annual level and at intra-molecular level. New methodological developments have been made during the last decade that have shown high potential in this respect. These developments enable us to study isotopic fractionation processes and environmental signals in $\delta^{13}C$, $\delta^{18}O$ and to some extent also in δ^2H values at molecular (compound-specific isotope analysis, "CSIA") and even at intramolecular (position-specific isotope analysis) level. Combined with methodological advancements in intra-annual tree-ring analysis (application of UV-laser), these new applications will improve our understanding of the relationships between climatic and isotope variability in tree rings. This chapter describes the new methodological developments of stable isotope analysis established for non-structural carbohydrates and tree rings.

7.2   Compound-Specific $\delta^{13}C$ and $\delta^{18}O$ Analysis of Sugars and Cyclitols

CSIA was introduced already in 1984 for $\delta^{13}C$, which was accomplished by coupling on-line Gas Chromatography (GC) to an Isotope Ratio Mass Spectrometer (IRMS) (Barrie et al. 1984). However, $\delta^{13}C$ analysis of carbohydrates using a GC/combustion-IRMS requires substantial derivatization, which incorporates external carbon atoms into the molecule and can cause kinetic isotope effects (Boschker et al. 2008; Macko et al. 1998). The development of a new interface for on-line coupling of high-performance liquid chromatography (HPLC) to an IRMS by Krummen et al. (2004) overcame these issues by removing the need for sample derivatization. Hence, it has become the method of choice for $\delta^{13}C$ analysis of sugars and sugar-like compounds (Boschker et al. 2008; Rinne et al. 2012). $\delta^{18}O$ analysis of carbohydrates has been recently achieved with GC/pyrolysis-IRMS (Zech and Glaser 2009; Zech et al. 2013a), where CSIA has been finally accomplished without the introduction of external O into the derivative (Lehmann et al. 2016). So far, no literature has been

published on compound-specific hydrogen isotope analysis of carbohydrates using chromatographic separation, presumably because of the oxygen-bound hydrogen that exchanges with surrounding water during sample processing or the addition of external hydrogen to the sugar molecule during derivatization.

7.2.1 $\delta^{13}C$ Analysis of Tree Sugars and Cyclitols Using Liquid Chromatography

Tree-ring $\delta^{13}C$ composition does not directly record changes in the ratio of leaf internal to ambient CO_2 concentrations (c_i/c_a), which would relate to changes in environmental conditions and their impact on photosynthetic rate and stomatal conductance (Barbour and Song 2014; Cernusak et al. 2009; Gessler et al. 2014). A multitude of mechanisms have been proposed that may modify the original environmental signal imprinted in primary photosynthates (Farquhar et al. 1982) during the pathway from leaf sucrose production to its consumption for stem wood production. These include respiration, enzymatic isotope fractionation, carbohydrate storage effects and fractionation during xylem cell formation (Gleixner et al. 1998; Helle and Schleser 2004; Panek and Waring 1997; Rinne et al. 2015a) (see Chap. 13). Detailed understanding of post-photosynthetic fractionations and processes is necessary for improved interpretation of $\delta^{13}C$ signal in tree rings. To achieve a profound level of understanding for a single biochemical process, studies must be conducted on a molecular level. This is because individual compounds within the "bulk" matter may have a $\delta^{13}C$ signal that contains substantially different environmental or biochemical information. For tree rings, the need for CSIA was recognized quite early, and cellulose extraction is nowadays a common, and recommended practice in stable isotope laboratories developing tree-ring isotopic chronologies. For metabolic studies, isolation of other compounds, such as sugars, starch and organic acids, is also needed. This section discusses CSIA of sugars and sugar-like substances (cyclitols), which are involved in various biochemical processes and are essential for the accurate interpretation of the tree-ring $\delta^{13}C$ archive.

7.2.1.1 Analytical Methodology

Isotope analysis of bulk material, such as whole leaves or bulk compounds extracted by water, has been the mainstay in biochemical studies. However, bulk isotope ratios reflect the average value of compound-specific isotope ratios in a mixture, where the individual compounds may substantially differ in their isotopic value due to differences in their genesis. Hence, the recent literature has started to explore the application of chromatographic separation on bulk matter prior to isotope analysis, which is possible on-line using high-performance liquid chromatography (HPLC), ion chromatography (IC) or gas chromatography (GC) connected via an interface to

an IRMS. HPLC and IC separation are best suited for the analysis of non-volatile, polar and thermally labile sugars and cyclitols (e.g. pinitol and myo-inositol), because no modifications (i.e. derivatization) are required for the analyte prior to its introduction to an HPLC/IC-IRMS system. For HPLC (Krummen et al. 2004) and IC (Morrison et al. 2010) separation, a small amount of purified sugar extract is injected into a moving stream of liquid (i.e. mobile phase, dilute NaOH), which passes through a column packed with particles of stationary phase. The most commonly used column for CSIA of sugars has been the Dionex CarboPac PA20 (Thermo Fisher Scientific) due to its capabilities at separating individual chromatography peaks (Boschker et al. 2008; Rinne et al. 2012). Column oven temperatures of 15 or 20 °C have been typically used for plant sugars (Rinne et al. 2015a). At higher temperatures isomerization will distort $\delta^{13}C$ values of hexoses (Rinne et al. 2012). Different compounds pass through a column at different times, i.e. they have different elution rates. The eluting compounds are oxidized to CO_2, when still in the mobile phase, using sodium persulfate ($Na_2S_2O_8$) under acidic conditions (H_3PO_4) at 99 °C. Since oxidization is done in the mobile phase, which contains dissolved CO_2 and a high abundance of O atoms from the chemicals used, these instruments are not suitable for compound-specific $\delta^{18}O$ analyses (for $\delta^{18}O$ analysis see Sect. 7.2.2). For $\delta^{13}C$ determination, the CO_2 produced from each carbohydrate is separated from the mobile phase in a capillary gas separator flushed with helium gas, dried and led to the IRMS for analysis. The analytical instruments enable accurate and reproducible $\delta^{13}C$ measurements of sample sizes down to 400 ng of C per compound. In addition, the produced CO_2 can be also used to obtain the concentration of each carbohydrate. An example of a HPLC-IRMS chromatogram of larch needle sugars is presented in Fig. 7.1.
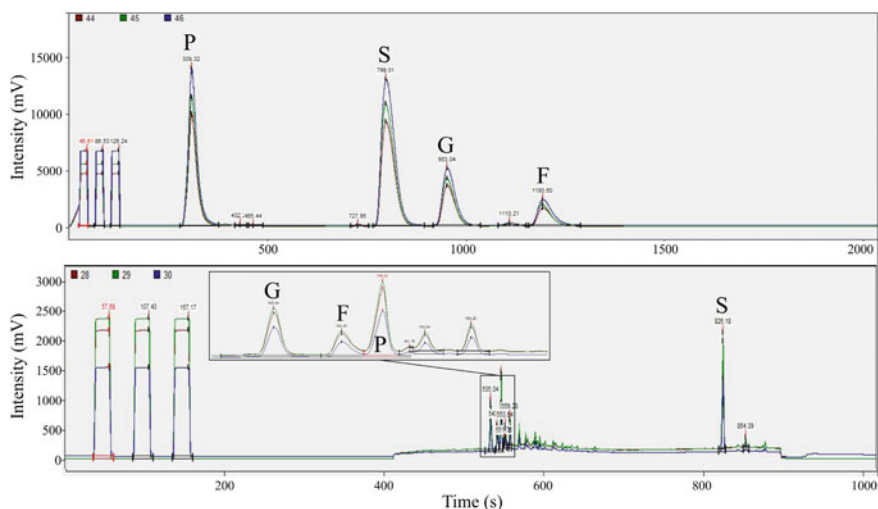

Fig. 7.1 Larch needle sugar HPLC-IRMS (top graph) and GC/Py-IRMS (bottom) chromatograms for compound-specific $\delta^{13}C$ and $\delta^{18}O$ analysis, respectively. The four compounds with adequate amount of material for isotope analysis are pinitol (P), sucrose (S), glucose (G) and fructose (F)

7.2.1.2 Sample Preparation

In the field, collected plant samples for sugar extraction are placed immediately in a cold box below 0 °C and microwaved soon after (60 s at 600 W) to stop enzymatic activities (Wanek et al. 2001). Sampled tissues are subsequently dried for 24 h at 60 °C and ground to fine powder. Typically, the water soluble fraction is extracted using a method modified after Wanek et al. (2001) and Rinne et al. (2012). According to this method, reaction vials are filled with 60 mg of the homogenized needle powder and 1.5 mL of Milli-Q water (18.2 MΩ, total organic C < 5 ppb). The mixture is stirred with vortex until the powder is fully suspended. The tubes are then placed in a water bath at 85 °C for 30 min. The samples are then centrifuged at 10,000 g for 2 min. For phloem samples, the exudation method has been used for obtaining sugars for isotope analysis (Gessler et al. 2004; Treydte et al. 2014), and described in detail in Chap. 13. After extraction, neutral carbohydrates are purified from ionic compounds using anion and cation exchange cartridges (Fionex OnGuard II H and OnGuard II A, Thermo Fisher Scientific; Wild et al. 2010) and from phenolic compounds (Dionex OnGuard II P) as described in detail in Rinne et al. (2012). Purification is necessary not only to simplify the chromatogram but also to remove compounds that could affect the column performance and lifetime (Boschker et al. 2008).

7.2.1.3 Research Applications

So far only a few studies have been published on compound-specific $\delta^{13}C$ analysis of tree sugars and cyclitols. CSIA has been applied on leaf (Bogelein et al. 2019; Churakova (Sidorova) et al. 2018; Churakova (Sidorova) et al. 2019; Galiano et al. 2017; Rinne et al. 2015a), twig and stem phloem (Bogelein et al. 2019; Smith et al. 2016), shoot (Streit et al. 2013) and coarse root (Galiano et al. 2017) samples for tree physiological and environmental studies, both at natural isotope abundance and after $^{13}CO_2$ labelling. In addition to trees, CSIA of sugars has been used on a CAM plant *Kalanchoë daigremontiana* to study the flux of carbon from PEPC and direct Rubisco fixation (Wild et al. 2010), on potato plants to study source of leaf respired CO_2 (Lehmann et al. 2015) and on common bean to determine the influence of sugars and cyclitols on predictions of plant water use efficiency (Smith et al. 2016).

For leaf sugars of larch (*Larix gmelinii* Rupr. in Siberia and *Larix decidua* Mill. in Swiss mountains), high resolution sampling during a growing season has shown a significant climatic signal with little or no sign of the use of carbohydrate reserves in $\delta^{13}C$ values of sucrose or hexoses (glucose and fructose) in studies at natural abundance (Churakova (Sidorova) et al. 2019; Rinne et al. 2015a). Also, Streit et al. (2013) combined ^{13}C-labelling with subsequent CSIA on larch (*Larix decidua*), and showed that sucrose $\delta^{13}C$ value was not much affected by old stored carbon. The intra-seasonal low-frequency trends of climatic variability observed in leaf sucrose, which is the sugar transported from leaves to phloem (Dennis and Blakeley 2000; Streit et al. 2013), of *Larix gmelinii* (Rinne et al. 2015a) were retained in the corresponding intra-annual tree-ring $\delta^{13}C$ records (Rinne et al. 2015b). This matching of seasonal signals

may indicate a better chance to reconstruct seasonal climate information from larch trees compared with other species that have shown more dependency on reserves. To improve knowledge on the use of C reserves for leaf sugar formation and to determine how the intra-seasonal climate signal in leaf sugars is preserved in intra-annual tree-ring $\delta^{13}C$ record, similar studies are needed also for other tree species and for different growing conditions.

CSIA analysis has shown that individual sugars and sugar-like compounds have differences in the environmental signal stored in their $\delta^{13}C$ values due to differences in their genesis (Fig. 7.2). In contrast to sugars, which have been reported to record well day-to-day variability of the ambient weather conditions (Rinne et al. 2015a), leaf pinitol is isotopically relatively invariable from one day to another suggesting a slow turnover rate for this compound (Bogelein et al. 2019; Churakova (Sidorova) et al. 2019; Rinne et al. 2015a). A significant carbon reserve signal in pinitol $\delta^{13}C$ was suggested also by the study of Streit et al. (2013). Yet, the abundance and $\delta^{13}C$ value of pinitol have been observed to correlate with stress-related processes, such as drought and cold temperatures (Churakova (Sidorova) et al. 2019; Ford 1984; Moing 2000; Rinne et al. 2015a). In addition to the significant differences in intra-seasonal trends between pinitol and sugars, also the absolute $\delta^{13}C$ values differ: pinitol is in general relatively ^{13}C-depleted. For these reasons, climatic and physiological signals
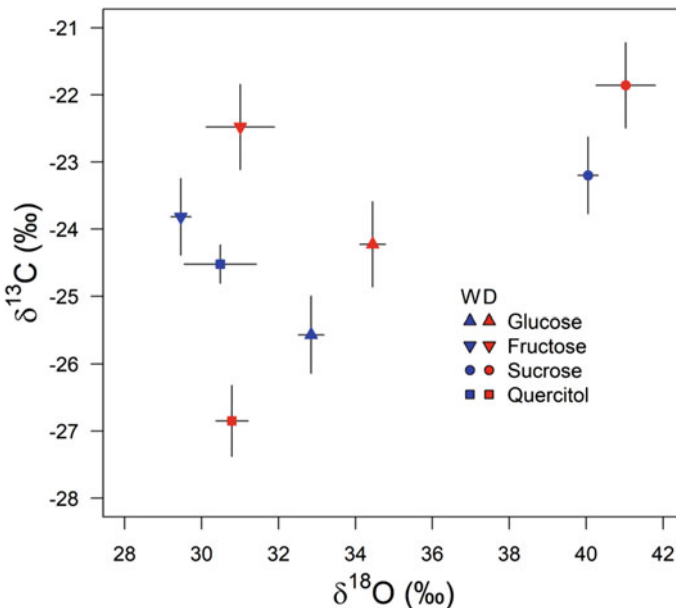

Fig. 7.2 CSIA of individual leaf sugars. $\delta^{13}C$ and $\delta^{18}O$ values in glucose, fructose, sucrose, and quercitol in 2 year old oak (*Quercus robur*) saplings under well-watered (W) and dry (D) soil moisture conditions measured by HPLC- and GC/Pyr-IRMS, respectively. Dry conditions were induced by no water addition for 3 weeks. Experimental details of the greenhouse experiment can be derived from (Lehmann et al. 2018). Mean ± SE (n = 4–5)

extractable from leaf photosynthates can be reduced or even distorted, if bulk $\delta^{13}C$ analysis (vs. CSIA) is used for samples with high pinitol content. For example, (Bogelein et al. 2019) reported absence of diel variation in $\delta^{13}C$ of leaf and twig phloem water soluble organic matter of Douglas fir, which was connected with the large amount of isotopically relatively invariable cyclitols. Further, the CSIA studies of Rinne et al. (2015a) and Rinne et al. (2015b) on larch suggested that the widely reported and debated ^{13}C-depletion of leaf bulk sugars relative to tree rings (Gessler et al. 2009; Gleixner et al. 1993) is in large parts due to the high abundance of ^{13}C-depleted pinitol in the leaves, as well as due to the ^{13}C-enrichment of the transport sugar sucrose relative to hexoses (Bogelein et al. 2019; Churakova (Sidorova) et al. 2018; Churakova (Sidorova) et al. 2019; Rinne et al. 2015a). Bulk sugar $\delta^{13}C$ analysis can also lead to erroneous conclusions on the use of reserves for leaf sugar formation, if pinitol is abundant in the studied leaves, as is typical for areas with cold winters where pinitol is needed for cryoprotection (Lipavská et al. 2000).

The ^{13}C-enrichment of leaf sucrose relative to hexoses is likely caused by invertase enzyme (Rinne et al. 2015b), which causes fractionation at the C-2 position of fructose leading to ~1‰ relative enrichment of sucrose (Gilbert et al. 2011; Mauve et al. 2009). The $\delta^{13}C$ difference between leaf sucrose and hexoses can be sustained with continuous synthesis (hexoses) and transport (sucrose) reactions (i.e. branching points) (Hobbie and Werner 2004). However, the level of leaf sucrose ^{13}C-enrichment relative to hexoses is not constant in the published studies (Bogelein et al. 2019; Churakova (Sidorova) et al. 2018; Churakova (Sidorova) et al. 2019), not even within a growing season (Rinne et al. 2015a). This may indicate, for example, a varying level of activity of the fractionating invertase enzyme (Rinne et al. 2015b), the presence of readily available residual remobilized carbohydrates (Rinne et al. 2015b), tree health status (Churakova (Sidorova) et al. 2018) or species specific differences (*Pinus mugo* ssp. *uncinata* and *Larix decidua*) (Churakova (Sidorova) et al. 2019).

The ^{13}C-enrichment of sucrose relative to hexoses and cyclitols could also explain the reported ^{13}C- enrichment of phloem (where sucrose is loaded for downstream transport) relative to leaves in studies that have analysed bulk sugar $\delta^{13}C$ values (Brandes et al. 2006). Indeed, for Douglas fir trees (*Pseudotsuga menziesii*), Bogelein et al. (2019) reported a one-to-one relationship between leaf sucrose $\delta^{13}C$ and twig bulk sugar $\delta^{13}C$ values supporting the hypothesis. However, for broad-leaved species, compartmentalization of sugars with different $\delta^{13}C$ composition in leaf mesophyll may induce an additional isotopic fractionation during phloem loading (Bogelein et al. 2019). More studies are needed to understand how leaf-to-phloem isotope fractionation differs between tree species. Further isotopic discrimination may occur during tree-ring formation due to the kinetic isotope effect of invertase, if a branching point is present also during wood formation (Rinne et al. 2015b). Concomitant CSIA analysis of sugars obtained from different tree compartments on a seasonal scale combined with high-resolution tree-ring analysis are needed to construct isotope fractionation transfer models, including storage and later remobilization. This will lead to a better knowledge of the formation of tree-ring isotope signal enabling utilization of tree-ring isotope chronologies at their full potential.

7.2.2 $\delta^{18}O$ Analysis of Tree Sugars and Cyclitols Using Gas Chromatography

During the last decade, several gas chromatograph pyrolysis IRMS (GC/Pyr-IRMS) methods have been developed for $\delta^{18}O$ analysis of individual carbohydrates (Lehmann et al. 2016; Zech and Glaser 2009; Zech et al. 2013a). The primary aim of each method is to convert the very hydrophilic carbohydrates into volatile and hydrophobic compounds by chemical conversion, a process which is commonly known as "derivatization". All common derivatization reactions for $\delta^{18}O$ analysis of individual carbohydrates permanently add new functional groups to oxygen atoms of the hydrophilic hydroxyl groups (i.e. C–OH) of carbohydrate molecules. The ideal method avoids oxygen isotope fractionation and addition of new oxygen isotopes during the derivatization reaction. The methylboronic acid (MBA) derivatization allows $\delta^{18}O$ analysis of individual carbohydrates derived from hemicellulose such as arabinose, xylose, rhamnose, or fucose (Zech and Glaser 2009), which was widely applied on plant hemicellulose in soils and thus for (paleo-)climate reconstructions (Hepp et al. 2016; Zech et al. 2013b). However, the MBA derivatization does not work with recent photosynthetic assimilates such as hexoses or sucrose. A trimethylsilyl (TMS) derivatization method produces more reliable $\delta^{18}O$ results for sucrose and raffinose, but not for hexoses and cyclitols (Zech et al. 2013a). The most recent method for compound-specific $\delta^{18}O$ analysis of carbohydrates is the methylation derivatization, which was found to produce precise and accurate $\delta^{18}O$ results for a wide variety of sugars (Lehmann et al. 2016). This includes common plant sugars, such as glucose, fructose, sucrose and cyclitols, as well as levoglucosan, a biomarker for biomass (e.g. wood or grass) burning. Therefore, the method has been widely applied in plant ecophysiological research (Blees et al. 2017; Lehmann et al. 2016, 2017, 2018, 2019).

In general, a minimum of about one milligram of sugars from plant material should be used for methylation derivatization to achieve adequate amount oxygen for $\delta^{18}O$ analysis. An addition of silver oxide, methyl iodide, acetonitrile, and dimethyl sulfide starts the (overnight) methylation process. After a centrifugation step, the methylated sugars in acetonitrile can be injected into a hot injector (250 °C) for separation on a GC column (e.g. SemiVolatiles, 60 m × 0.25 mm × 0.25 μm, Zebron, Phenomenex, Torrance, CA, USA). The GC is coupled via an IsoLink interface and a reference control unit to an IRMS (all Thermo Fisher Scientific, Bremen, Germany). The IsoLink holds space for a 32 cm oxygen isotope reactor (0.8 mm outer diameter) consisting of outer ceramic and an inner platinum tube filled with nickel wires. The reactor is heated to 1280 °C in a high temperature conversion oven causing pyrolysis of individual methylated sugars that elute from the GC and pass the reactor in a flow consisting of helium (1.4 mL min^{-1}) and 1% hydrogen in helium (ca. 0.6 ml/min). The oxygen isotope ratio of each individual sugar is then measured on the produced CO gas peak (mass 28/mass 30) using an IRMS (Fig. 7.1). Importantly, triplicates of standard sugar mixes of different concentrations should be interspersed into a measurement sequence for drift, amount, and pyrolysis offset corrections.

7.2.2.1 Sample Preparation for GC/Pyr-IRMS

Sample preparation including hot water extraction from plant material and sugar purification with ion-exchange cartridges generally follows the protocol of Sect. 7.2.1.2 in this chapter. However, a few points should be additionally considered for $\delta^{18}O$ analysis. (1) For a better understanding of oxygen isotope fractionations in plants, it is important to have also the information on $\delta^{18}O$ values of water in leaves and other tissues. Plant samples should therefore be ideally transferred into gas-tight glass vials (Labco, UK) and stored as cold as possible in the dark shortly after sampling to avoid metabolic activity. The vials allow the extraction of water by vacuum distillation (West et al. 2006) and the remaining dry material can be milled to powder and used for sugar extraction and purification (Lehmann et al. 2018). (2) Although oxygen isotope exchange between water and sugars have been observed to be negligible for the above-described sugar sample preparation (Lehmann et al. 2017), it is recommended to keep water extracts and purified sugars frozen at all times, if they are not used for further analysis. (3) Furthermore, prior to derivatization, it is generally recommended to freeze-dry each sugar sample to remove excess water, avoiding any potential isotope fractionation that can be caused by oven-drying (Lehmann et al. 2020).

7.2.2.2 Research Application ($\delta^{18}O$ of Individual Sugars)

Given the relatively new methodological development, research applications of the compound-specific $\delta^{18}O$ analysis of individual sugars in ecophysiological or dendrochronological research are still rare (Blees et al. 2017; Lehmann et al. 2016, 2017, 2018; Zech et al. 2013a). First applications on leaves from grasses and trees showed that sucrose is generally ^{18}O-enriched compared to hexoses and cyclitols. In grasses, biosynthetic fractionation factors (ε_{bio}) of ~33 and ~30‰ were found for sucrose and hexoses (Lehmann et al. 2017), respectively, both exceeding the commonly reported value of 27‰ (Sternberg and DeNiro 1983). Moreover, the ε_{bio} values of the individual sugars were found to depend on changes in relative humidity, and this dependence was stronger for sucrose than for other carbohydrates (Lehmann et al. 2017). The ε_{bio} was also found to be species dependent, so that ε_{bio} was higher in larch than in oak trees under similar environmental conditions. The results indicate that processes controlling the imprint of the leaf water isotopic signal on carbohydrates can differ with environmental conditions and between tree species, which should be considered in studies comparing $\delta^{18}O$ responses across sites and species (Treydte et al. 2007).

Leaf water, which reflects the synthesis water for carbohydrates, was found to be increasingly ^{18}O-enriched from the bottom to the tip or from the vein to the margin of a leaf (Cernusak et al. 2016). The extent of this ^{18}O-enrichment in leaf water has been observed to increase with a decrease in air humidity (Cernusak et al. 2016; Helliker and Ehleringer 2002). In addition to this ^{18}O-enrichment, the relative location of sucrose and hexose syntheses may differ within a leaf, e.g. higher sucrose

synthesis rates have been observed in tips of a grass leaf blade compared to the bottom (Williams et al. 1993). Thus, relatively higher synthesis rates of sucrose in ^{18}O-enriched leaf water compartments might therefore explain the ^{18}O-enrichment of sucrose compared of hexoses and thus oxygen isotope fractionations among individual carbohydrates (Lehmann et al. 2017). If true, a similar mechanism might explain the tree-specific $\delta^{18}O$ differences in carbohydrates between larch and oak. Relatively higher sugar synthesis in ^{18}O-depleted leaf water in the bottom of a needle may cause lower $\delta^{18}O$ values in leaf sugars compared to those in broadleaf oaks. In fact, the differences in leaf sugars are likely translated to tree-rings and should be considered if species responses to environmental changes are compared.

In contrast, only a few $\delta^{18}O$ data are currently available for cyclitols, also known as sugar alcohols or alditols (Lehmann et al. 2016). Overall, $\delta^{18}O$ values in sugar alcohols tend to be lower compared to sucrose and hexoses across different tree species. As described above (Sect. 7.2.1.3), biochemical pathways for sugar alcohols are different and their seasonal turnover is slower compared to photosynthetic assimilates. For instance, rapid changes in the isotopic composition of leaf water are only barely incorporated into cyclitols compared to other photosynthetic assimilates (Lehmann et al. 2017, 2018). High abundances of cyclitols, such as pinitol or quercitol, can therefore strongly dampen the $\delta^{18}O$ response of leaf sugars to recent environmental changes, if measured with standard $\delta^{18}O$ analysis for total organic matter (Kornexl et al. 1999a, b).

The different response of sugars and cyclitols in leaves to environmental stress can be deduced from Fig. 7.2. In a greenhouse experiment, 2 year old oak trees were kept for 3 weeks without water to induce drought stress, while a control was well-watered (see Lehmann et al. 2018 for experimental details). The drought stress caused no change in $\delta^{18}O$ values but lower $\delta^{13}C$ values in the cyclitol quercitol, while $\delta^{13}C$ and $\delta^{18}O$ values increased in sucrose and hexoses. These differences between cyclitol and sugars would have opposite physiological interpretations for dual isotope applications (Chap. 16) where the isotopic response of quercitol would be interpreted as lower assimilation rates without a change in stomatal conductance, and the isotopic response of sucrose and hexoses would indicate no change in assimilation rates but lower stomatal conductance (Scheidegger et al. 2000). Compared to the cyclitol quercitol, the isotopic response of sucrose and hexoses likely reflects the more realistic physiological adaptation to the drought treatment, given that no water was given for 3 weeks and the oak saplings had to close their stomata to avoid unwanted water loss. Thus, our result demonstrates that high amounts of cyclitols in a sample may lead to dampened or falsified isotopic responses to environmental stresses, if only bulk sugar fractions are measured, and therefore may cause misleading interpretations. Compound-specific isotope analysis of sugars allow to avoid these biases as the isotopic response of indivudal compounds is specificly measured.

Further studies showed that individual sugars were up to 8‰ enriched in [18]O compared to cellulose in grass leaves under controlled conditions, with $\delta^{18}O$ values of sucrose showing the highest correlation with those of cellulose among other individual sugars (Lehmann et al. 2017). This indicates a strong biochemical link between sucrose and cellulose synthesis, but also a strong ^{18}O-depletion of sugars during

cellulose synthesis (Cernusak et al. 2005; Farquhar et al. 1998; Roden et al. 2000). Moreover, sucrose has been observed to better integrate rapid isotopic changes in leaf water than other carbohydrates (e.g. hexoses, cyclitols) (Lehmann et al. 2018, 2019). Sucrose might therefore be the ideal candidate to trace $\delta^{18}O$ variations from leaves to stem cambium cells where tree-rings are produced. However, studies on a compound-specific level tracing the translocation of sucrose in the phloem to sink tissues, such as tree-rings, are very scarce and limited so far to leaf and twig level (Cernusak et al. 2003; Lehmann et al. 2018). The compound-specific approach may therefore be applied on twig and stem phloem in mature trees to better understand how the isotopic signal in leaves is transported and incorporated into tree-ring archives (Gessler et al. 2013; Treydte et al. 2014).

In summary, the newest findings by CSIA studies reveal high $\delta^{18}O$ variation between individual sugars, which can be much higher than year-to-year variations in tree-ring cellulose. The leaf water signal is differently incorporated by different sugars (e.g. sucrose vs. hexoses versus cyclitols) and depends on environmental conditions (e.g. relative humidity, drought) and species. The recent CSIA results are particularly important for modelling studies, which aim to reconstruct the leaf water isotopic enrichment and thus the physiological responses to environmental conditions from tree-ring isotope ratios. Studies comparing tree-ring $\delta^{18}O$ values of different species and/or across different sites should also consider these newest developments.

7.3 UV-Laser Aided Sampling and Isotopic Analysis of Tree Rings

Two new approaches to tree-ring stable isotope analysis have been established, which both utilize UV-laser systems. One of them is UV-laser assisted microdissection, which can be used to cut subsamples of tree rings that are subsequently manually prepared for isotopic analysis using the conventional methods (e.g. cellulose extraction, EA/HTC-IRMS analysis). The other UV-laser-based method enables on-line isotope analysis of tree rings, which is accomplished via laser ablation (as opposed to laser cutting). Both methods take advantage of the features of modern UV-laser systems, which support the sampling of tree tissues at a very high spatial resolution and accuracy.

7.3.1 UV-Laser Microscopic Dissection (LMD) of Tree Rings

UV-laser-assisted microdissection (LMD or LAM) or laser capture microdissection (LCM) is a technology allowing for isolating areas of interest from cell tissues under direct microscopic visualization. LMD systems are typically used for isolating

DNA and RNA in e.g. genomics, transcriptomics, metabolomics and next generation sequencing, as well as for live cell culture manipulation in cloning and re-cultivation experiments (c.f. Leica Microsystems GmbH 2018; Carl Zeiss Microscopy GmbH 2013 for comprehensive lists of publications). A key advantage of using the LMD technique is on-screen selection of sample areas enabling accurate sub-seasonal sampling of single cell rows or dissection of complete tree rings with irregular shapes or narrow ring widths, as documented in recent studies (Blokhina et al. 2017; Kuroda et al. 2014; Schollaen et al. 2014, 2017). Furthermore, the technique provides electronic documentation of the dissection processes by photo or video sequences, as well as a report of labelled and dissected elements.

7.3.1.1 Instrumentation and Principle of the LMD Methodology

The LMD approach to dissecting and sampling wood cells of tree rings for downstream analysis has first been described in detail by Schollaen et al. (2014). Two different UV-laser microdissection microscopes (i) LMD7000 by Leica Microsystems GmbH, Wetzlar, Germany and (ii) PALM MicroBeam by Carl Zeiss Microscopy GmbH, Jena, Germany, implemented at the GFZ German Research Centre for Geosciences, Potsdam, were tested and their advantages and constraints of the use in tree-ring stable isotope research was discussed. The LMD systems are basically used off-line and generally consist of a microscope equipped with objectives of high UV transmission, a UV-laser cutting unit, a motorized stage for various sample holders and specimen collectors. Sample holders can carry thin sections of up to 50 mm × 76 mm in area and a variety of vials like PCR tubes or 96-well plates can be employed for receiving specimens from the dissection of the tree-ring samples.

The preparation and analysis scheme comprises five steps:

(1) manual preparation of thin wood cross-sections (max. 1500 μm thickness) with a microtome or a high-precision saw,
(2) microscopic identification and pen-screen selection of woody tissues of interest,
(3) automatic UV-laser-assisted microscopic dissection of inter-or intra-annual wood sections,
(4) automatic sample collection by gravity (Leica LMD 7000) or forceps (PALM Microbeam) into PCR tubes or 96-well plates, optional chemical treatment (e.g. cellulose extraction), and
(5) stable isotope analysis via conventional isotope ratio mass spectrometry (IRMS) coupled online to a combustion or pyrolysis furnace (δ^2H, $\delta^{13}C$ and $\delta^{18}O$).

In general, wood samples of 100–1500 μm thickness can be dissected without any major constraints. The use of cross-sections thinner than 100 μm may not be advised. Wood of certain tree species, e.g. *Adansonia digitata* (baobab) can have densities varying between 0.09 and 0.2 mg/mm^3. The density of cellulose extracted from conifers can be in a similar range. Specimen dissected from corresponding

cross sections of about 0.15 mm^3 (e.g. from a 0.3 × 5 mm wide and 0.1 mm thick cross-section) yield a mass range of 13.5–30 µg, which can be challenging for routine mass spectrometry with conventional combustion/pyrolysis systems. Dissection of samples of up to 1500 µm thickness requires a number of cutting iterations to be preselected in the LMD software resulting in automatic adjustment of the in-focus depth of the Z-axis of the UV-laser beam during repeated lasering of the pre-defined cutting line. Unlike UV-ablation lasers, LMD systems are producing sharp-contoured pieces of sample tissue instead of wood dust.

Relevant plant cells/tissues can be selected on-screen, while non-relevant tissues (e.g. resin ducts, wood rays) may not be selected or be removed, i.e. cut away before sampling. Any size and area within the given range of the size of the sample holder (max. 50 mm × 76 mm) can be dissected. This allows for the precise dissection of asymmetric tree rings or parts thereof, for example by lobate growth, intra-ring density fluctuations or wedging tree rings. Furthermore, it is possible to cut serial sections or even to pool sample material, for example, if the weight of the dissected tissue from one thin section is found insufficient for a stable isotope measurement (for details c.f. Schollaen et al. 2014, 2017). Sample material from the same array of wood cells can be identified unambiguously on a second or third cross-section and may be pooled for chemical treatment, e.g. cellulose extraction before IRMS analysis. However, thin wood cross-sections may also be subject to LMD after cellulose extraction. (Schollaen et al. 2017) showed that tree-ring structures of cellulose laths, which represented a variety of tree species (coniferous and angiosperm wood) with different wood growth rates and differently shaped tree-ring boundaries, largely remained well identifiable and suited for UV-dissection at annual and intra-annual resolution. Nevertheless, it can be challenging to work with cellulose cross sections originating from very soft and light wood like e.g. from baobabs (*Adansonia digitata*), which contain a high percentage of parenchyma tissue (up to 80%) (Schollaen et al. 2017). In order to get enough sample material for a stable isotope measurement, either the radial cutting width or the thickness of the thin section needs to be adjusted accordingly. A wider sample reduces the possible data points per tree ring, whereas a thicker sample increases the time required to dissect the sample. For example, ten cutting processes on the same sample were needed to successfully separate a baobab cellulose sample from a cross section of 1300 µm thickness.

7.3.1.2   Comparison of the LMD Systems and their Operation

The two commercially available LMD systems differ concerning their practical implementations and applications. The laser from Leica is moved via optics and the cross-section samples are mounted on a stage that is fixed during actual laser cutting. The Leica system uses high precision optics to steer the laser beam by means of prisms along the desired cut lines on the tissue. Limitations of earlier software (v6.7.1.3952; Schollaen et al. 2014) have been overcome, so that the laser cutting of the LMD7000 is no longer restricted to the actual microscopic field of view. Larger areas, for example whole tree rings, can now be marked. The dissected sample tissues

principally fall down by gravity into collection vessels like 96-well plates, which can be equipped with tin or silver capsules for direct uptake of sample tissue. Thus, samples can be prepared directly for conventional autosampler systems coupled to IRMS. Another limitation of the Leica system was the lack of an automatic z-focus adjustment to allow repeated laser cutting of thicker cross-sections (Schollaen et al. 2014) but this function has been available since 2017.

Compared to the Leica microscope, the objectives of the Zeiss microscope are installed inversely, or underneath the sample holder, i.e. dissected specimen cannot be collected by gravity. Hence, tissues of interests are marked via mouse or screen pen on the lower sample side and can be selected beyond the visible screen. The laser stays fixed while the sample is moved by the high-precision stage during the dissection process. The UV laser passes through the glass slide and the dissected sample tissues remain in position. After all of the marked tissue has been dissected, specimens are picked up manually with a forceps and transferred into tin or silver capsules for stable isotope measurements. Dissected tree-ring sample tissues were observed to be too heavy for patented ZEISS laser catapult that was designed to toss upwards individual cells or even smaller specimen up into collection vessels (Schollaen et al. 2014). The Zeiss system also comes with an automatic z-focus feature that allows easy definition of the number of automatic cutting iterations. As the Zeiss laser (100 µJ, wavelength 355 nm) is less powerful than the laser from Leica (120 µJ, wavelength 349 nm), more cutting iterations are generally required.

Together with the manual collection of dissected specimens, the overall sampling process with the Zeiss system takes longer than with the Leica system. In general, the use of UV-laser microdissection microscopes is not necessarily faster than traditional methods for the dissection of wood tissue. The cutting process of selected tissue lasts ca. 1–2 min, depending on the size of the selected area, the thickness of the cross-section, density of the wood material and the UV laser settings. If further cutting iterations are required, more time is needed. The average sample throughput per 8-h day may vary between 20 and 120 samples. This includes the on-screen selection of area, the automatic UV-laser-based microscopic dissection and the collection of specimens, as well as unpredictable interferences such as stuck specimens (Leica LMD7000). With some modification of the current sample collection methods the Leica system could be run automatically overnight, which would increase sample throughput drastically, allowing more cuts than manual methods.

7.3.2   On-line Analysis of Tree-Ring $\delta^{13}C$ by Laser Ablation IRMS

Laser ablation-combustion-gas chromatography-IRMS method (hereafter LA-IRMS) to analyze carbon isotope composition of wood was introduced by Schulze et al. (2004). In the method, the labor intensive process of sectioning wood manually or by microtome to produce samples for intra-annual isotope studies (Helle and

Schleser 2004; Kagawa et al. 2003) is replaced by a spatially precise, high resolution sampling of tree rings in situ using a UV-laser (Schulze et al. 2004). In contrast to the newly developed LMD technique (see Sect. 7.3.1.), the LA-IRMS combines the sampling and isotope analysis by transportation of the ablated sample material directly to IRMS via a modified combustion unit (Loader et al. 2017; Schulze et al. 2004). Unlike the LMD technique, the LA-IRMS applications have so far been limited to δ^{13}C analysis.

7.3.2.1 Instrumentation and Principle of Analysis

Similar to a conventional EA-IRMS, which is used for "bulk" isotope analysis of, for example, tree rings, a LA-IRMS operates as a continuous flow IRMS (Schulze et al. 2004). A wood sample is placed in a He-flushed chamber connected to a UV-laser, where a subsample of the wood is removed by laser ablation, and the released particles are directed by the He flow to a miniaturized combustion unit. Water vapor is removed from the formed CO_2, which can then be introduced into a liquid nitrogen trap that concentrates CO_2 from a single ablation run in a small volume of carrier gas (Loader et al. 2017). The cryogenic trapping is beneficial for high resolution δ^{13}C analysis, where the amount of ablated wood is at the minimum (Rinne et al. 2015b). After the CO_2 is released from the cold trap, it is separated from other gaseous products in a GC-column prior to its introduction into an IRMS for δ^{13}C analysis (Loader et al. 2017; Schulze et al. 2004).

The size of the sample CO_2 peak detected by IRMS can be tuned by adjusting the laser output power settings, the laser spot size and the length of the ablated track (Loader et al. 2017; Schulze et al. 2004), which is positioned along a line parallel to the corresponding tree-ring boundary (Fig. 7.3). The ablation track is positioned using a camera connected with the laser unit and controlled by the laser software.
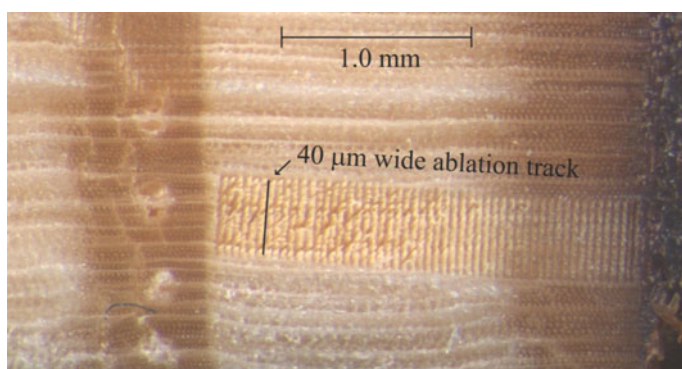

Fig. 7.3 Picture of an annual ring of larch (*Larix gmelinii* Rupr.) analysed using a LA-IRMS (modified after Rinne et al. 2015b). 53 laser ablation tracks with a 40 µm diameter laser spot size and 40 µm were analysed within the annual ring. The width of the annual ring was 2.3 mm.

A spatial resolution of 80 µm has been reached in LA-IRMS analysis using 40 µm diameter spot size for ablation tracks and 40 µm spacing between each track (Fig. 7.3; Rinne et al. 2015b, Schulze et al. 2004). The maximum number of ablation tracks (i.e. $\delta^{13}C$ data points) in an intra-annual tree-ring $\delta^{13}C$ profile depends on the width of the tree ring and on the selected laser spot size (Fig. 7.3).

Following the principle of identical treatment (Chap. 6), at least one or preferably three reference materials with known isotope composition should be measured with LA-IRMS together with the analytes for correcting the produced $\delta^{13}C$ results. Ideally, the reference material should be matrix matched to the sample and isotopically homogenous to a very fine spatial scale. Unfortunately, certified reference materials of this type do not exist, and as a substitute, the IAEA-C3 cellulose paper has been used (Loader et al. 2017; Schulze et al. 2004). Analysis of this material has shown that the precision of LA-IRMS measurements (the standard deviation of repeated measurements (SD): 0.1–0.2‰; Loader et al. 2017; Schulze et al. 2004) is comparable to conventional EA-IRMS $\delta^{13}C$ measurements (SD: $^{\leq}0.1‰$). However, a $\delta^{13}C$ offset correction may be required for tree-ring LA-IRMS data to correct for a matrix effect caused by using a non-matrix-matched reference material, such as the cellulose IAEA-C3 (Míková et al. 2014; Rinne et al. 2015b).

7.3.2.2   Sample Preparation for LA-IRMS

Due to the mobility of resin in tree rings (Long et al. 1979), resinous tree cores obtained from conifers should be treated in a Soxhlet apparatus with hot ethanol over a period of 50 h followed by repeated washing with boiling deionized water to remove the solvents completely (Loader et al. 2017; Rinne et al. 2015b). Tree cores can then be dried at 40 °C in an oven for 2 days to speed up the drying process (Rinne et al. 2015b). Despite of the Soxhlet extraction procedure, some resins have occasionally been observed to persist in resin ducts, as indicated by ATR-FTIR analysis (Rinne et al. 2005) and deviant $\delta^{13}C$ values obtained during laser ablation (Loader and Rinne, unpublished data). Consequently, resin ducts should be avoided, when positioning ablation tracks, in case of incomplete resin removal (Rinne et al. 2015b).

For laser ablation, the surface of the analyzed tree-ring sample should be even to enable accurate focusing of the laser beam. This can be achieved by treating the wood surface with a microtome, razorblade or sandpaper (Loader et al. 2017; Schulze et al. 2004; Soudant et al. 2016). Finally, the resin extracted (for conifers) and polished sample is cut into sections that fit into the laser chamber together with the reference material. LA-IRMS analysis of resin extracted wood takes advantage of the reported generally similar climatic signal in $\delta^{13}C$ values of wood compared to extracted cellulose (e.g. Helle and Schleser 2004; Schulze et al. 2004; Weigt et al. 2015). If the objectives of the study require the analysis of cellulose instead of resin-free wood, cellulose extraction can be performed prior to LA-IRMS using methods designed for whole wood sections as described in Loader et al. (1997) and Schollaen et al. (2017) (cf. Schulze et al. 2004). However, the extraction procedure will cause

some distortion to the wood sections (e.g. shortening and bending) (Schollaen et al. 2017; Schulze et al. 2004), which may complicate the selection of ablation spots as well as the connection of the individual $\delta^{13}C$ results with tracheid formation times, especially in very high resolution studies. See Chapter 5 for further details on chemical pre-treatments, review and discussion of the use of wood, resin extracted wood and cellulose in stable isotope studies.

7.3.3 Conversion of High Resolution Tree-Ring Isotope Data into a Temporal Scale

To fully utilize high resolution stable isotope data from tree rings, special consideration should be given on how to link tree-ring isotopic profiles obtained by LMD (δ^2H, $\delta^{13}C$ or $\delta^{18}O$) or LA-IRMS ($\delta^{13}C$) methods with other seasonal data that has been collected from the studied tree (e.g. carbohydrate dynamics of the growing season) and how to relate the isotopic profiles with climatic events (Schulze et al. 2004). To accomplish this, the isotopic profiles can be transformed into a temporal scale using direct (dendrometer band) or indirect (e.g. cell size, cell number) seasonal growth measurements of tree rings (Skomarkova et al. 2006; Walcroft et al. 1997; Vysotskaya et al. 1985). However, a tree-ring stable isotope signal is not formed only during the phenophase of wood expansion but also during the phase of lignification, whose start and end dates occur later in the growing season in comparison to those of the expansion phase (Cuny et al. 2013; Rinne et al. 2015b). Consequently, for laser-assisted, high resolution isotopic analysis of woody tissue, ideally both the seasonal expansion and lignification development of the tree ring should be determined.

Although somewhat laborious, periodical collection of micro-cores provides a way of monitoring wood formation stages without causing undue damage to the trees under study (Forster et al. 2000). Several methods of obtaining micro-cores exist, including different types of needles, punchers and miniaturized borers (Forster et al. 2000; Rossi et al. 2006). Samples are collected from the trees during the growing season (e.g. weekly) following an oblique pattern around the tree trunk (Fonti et al. 2018; Rinne et al. 2015b). Distance between coring spots should be ≥ 1 cm to avoid wood tissue affected by previous sampling (Forster et al. 2000). In the field micro-cores are placed in ethanol solution and subsequently stored in a fridge until further processing. Sample processing and analysis for xylogenesis parameter measurements is described in detail in (Schweingruber et al. 2006). Careful comparison of the laser ablation spots or laser dissection areas to tree-ring structure, together with the information on timing of tracheid formation obtained from micro-core time series, allows one to estimate the corresponding timing of each individual isotopic measurement within the calendar year (Fonti et al. 2018; Rinne et al. 2015b).

7.3.4   Research Applications

The laser assisted methods have provided an unprecedented spatial accuracy in sampling for isotopic analysis compared to conventional use of handheld instruments or microtomes (De Micco et al. 2012; Rinne et al. 2015b; Schollaen et al. 2014; Schulze et al. 2004). Both LMD and LA methods are capable of sampling very small scale features in tree rings, such as small growth defects (Battibaglia et al. 2010; De Micco et al. 2012) and ray parenchyma (Schollaen et al. 2014), and provide material for high resolution intra-annual isotope analysis (Bruykhanova et al. 2011; Fonti et al. 2018; Rinne et al. 2015b; Schollaen et al. 2014; Skomarkova et al. 2006; Soudant et al. 2016; Vaganov et al. 2009) either on-line (δ^{13}C: LA-IRMS) or off-line (LMD: δ^{13}C, δ^{18}O, δ^2H).

The studies utilizing laser assisted methods have combined the resulting knowledge of intra-annual δ^{13}C variability with other tree-ring characteristics that can be measured in equal spatial resolution, such as wood density (Schollaen et al. 2014; Skomarkova et al. 2006) and wood anatomical traits (Battibaglia et al. 2010; Bruykhanova et al. 2011; De Micco et al. 2012; Fonti et al. 2018; Vaganov et al. 2009), for the better understanding of intra-ring proxy signals. The isotopic profiles together with other seasonal data can then be compared with environmental variables for deepening our understanding about the mechanisms controlling the isotope variability in tree rings (see Chap. 15 for further discussions). The outcomes of such studies, where the UV-laser assisted analytical methods have been employed, include (1) evaluation of a dependency on carbohydrate reserves (Bruykhanova et al. 2011; Fonti et al. 2018; Rinne et al. 2015b; Skomarkova et al. 2006; Vaganov et al. 2009), (2) influence of stand structure (Skomarkova et al. 2006), tree age (Fonti et al. 2018) and tree growth rates (Vaganov et al. 2009) on the intra-annual δ^{13}C signal, (3) preservation of seasonal rainfall patterns in tree-ring δ^{18}O (Schollaen et al. 2014) and (4) linking of intra-annual tree-ring δ^{13}C profiles to upstream post-photosynthetic processes by analyzing the seasonal variation of δ^{13}C in different leaf sugars within growing seasons (Rinne et al. 2015b). In the future, these methods will continue to broaden our understanding of the fine scale variation of the isotopic composition of tree rings. In addition, LA-IRMS has potential for it to be used as a tool for selecting tree cores for conventional isotopic analysis, for analyzing exceptionally narrow rings and for constructing long δ^{13}C tree-ring chronologies in a relatively less labor intensive manner (Loader et al. 2017).

7.4   Position-Specific Isotope Analysis of Cellulose

Intra-molecular isotope analysis of tree-ring cellulose has been established for all the constituent chemical elements. For δ^2H and δ^{13}C analysis, the methodology utilizes the nuclear spin of ^{2}H and ^{13}C, which produces a nuclear magnetic resonance (NMR) signal that can be used for position-specific measurements. For δ^{18}O analysis, on the

other hand, a different approach has been necessary, since ^{18}O does not have a nuclear spin. The published methods involved for $\delta^{18}O$ requires a substantial amount of synthetic organic chemistry, which is needed to isolate or remove oxygen atoms from particular positions for $\delta^{18}O$ determination.

Significant intra-molecular isotope variation has been reported for cellulose, for all the three elements. If changes occur in the intra-molecular isotope pattern, this can influence the δ values of cellulose, but this influence cannot be inferred without intra-molecular isotope data. Applied to isotope studies of tree rings, trends in a δ value of cellulose might be attributed to changing climate, while the intra-molecular location of the effect would point to changes in metabolic regulation along the tree-ring series. Further, because intra-molecular variation is created by enzyme reactions, it can in principle carry ecophysiological information, as illustrated by Gleixner and Schmidt (1997). Researchers have barely begun to explore this potential wealth of information, largely because intra-molecular isotope variation was for a long time extremely cumbersome to measure.

7.4.1 Position-Specific δ^2H and $\delta^{13}C$

In tree-ring studies, stable isotope composition is measured for the whole molecule, that is, for the glucose units of cellulose. However, a glucose unit contains for each of the elements several intra-molecular positions, which are biochemically distinct. Thus, the question arises how these distinct positions behave in terms of isotope abundance. Kinetic isotope effects modify the abundance of heavy isotopes that are connected to a particular chemical bond. Because isotope effects of enzymes synthesizing glucose vary, it must be expected that isotope abundance varies among the intra-molecular positions. This conclusion holds for all isotopes in non-symmetrical molecules. Indeed, it has also been demonstrated for many other metabolites that stable isotope abundance varies among intra-molecular positions. This was concluded in an earlier study for ^{13}C in acetyl-CoA (De Niro and Epstein 1977) and later for deuterium (D) in several metabolites (Martin et al. 1992). For photosynthetic glucose, Rossmann et al. (1991) observed substantial intra-molecular ^{13}C variation, which could be explained mechanistically as equilibrium isotope effect of aldolase (Gleixner and Schmidt 1997). This example demonstrates an important advantage of intra-molecular isotope data: the intra-molecular localization of isotope fractionation directly suggests which enzyme might be responsible, and this hypothesis can then be compared to the enzyme's isotope effect or be tested in experiments.

For deuterium, Martin et al. (1992) summarized the knowledge on various metabolites. They describe intra-molecular δ^2H variation for sugars, amino acids and monoterpene biosynthesis, with typical intra-molecular variation of hundreds of ‰. For ^{13}C, the typical intra-molecular isotope variation is 10‰ (Schmidt 2003) (for intra-molecular oxygen isotope variation, see Sect. 7.4.2). From the size of this intra-molecular variation, it must be concluded that δ values are averages of the intra-molecular isotope data, with important consequences.

7.4.1.1   Sample Preparation and Analytical Methodology

Measurements of intra-molecular ^{13}C-abundance of glucose were first performed by controlled breakdown of the molecule and subsequent IRMS analysis of the fragments (Rossmann et al. 1991). However, such wet-chemical methods are extremely labour-intensive and need to be tailor-made for each metabolite. In the meantime, ^{13}C NMR has been established as a tool for intra-molecular ^{13}C-measurements. In a ^{13}C NMR spectrum, each structurally distinct C gives rise to a specific signal (Fig. 7.4). Careful optimization of parameters is needed so that the signal integrals reflect relative isotopomer abundances (Chaintreau et al. 2013), but when this is achieved, this general method has been applied to various metabolites including tree-ring cellulose (Romek et al. 2017; Wieloch et al. 2018). NMR has the fundamental advantage that the intra-molecular isotope composition of the intact molecule is determined, avoiding a risk for isotope fractionation during chemical breakdown, pyrolysis or fragmentation. On the other hand, NMR gives relative abundances of isotopomers, but no information about the ratio of heavy to light isotopes.

For measurements of intra-molecular ^{2}H variation, deuterium NMR spectroscopy has been the method of choice. NMR can be done both on solid and solution samples, but solution NMR achieves the resolution required for isotopomer analysis, therefore polymeric analytes such as cellulose have to be broken down first. Although the 7 carbon-bound deuterons of glucose in principle give separate NMR signals, these are in practice not resolved. Therefore, glucose must be converted into a derivative that gives resolved signals by locking the anomeric equilibrium and by lowering the polarity of the molecule so that it can be dissolved in low-viscosity organic solvents yielding narrow signals (Betson et al. 2006). As seen in Fig. 7.5, deuterium isotopomer variation is directly visible in the NMR spectrum. But as for ^{13}C, quantification of the isotopomers is done by integration of the signals by lineshape fitting. NMR spectra give ratios of isotopomer abundances, but do not directly reflect the ratio of heavy to light isotope. From isotopomer patterns, site-specific isotope ratios can be calculated in two ways: Either the δ^2H of the analyte is measured independently and isotope ratios for the intramolecular positions are calculated by isotope
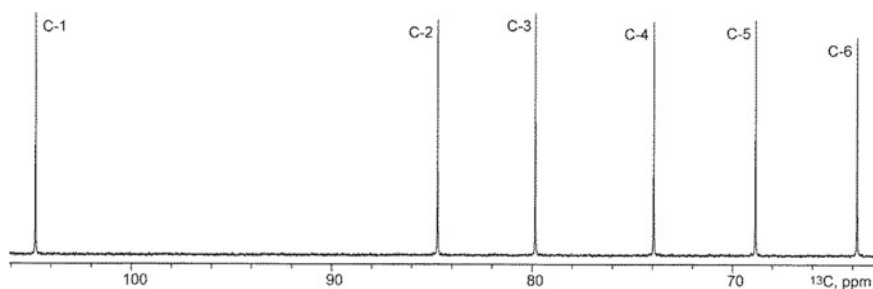

Fig. 7.4 ^{13}C NMR of a glucose derivative. Each signal originates from one ^{13}C isotopomer. The x-axis is the so-called chemical shift. The "ppm" units are unrelated to isotope abundance but describe the signal positions that are governed by the intra-molecular chemical environment of each ^{13}C
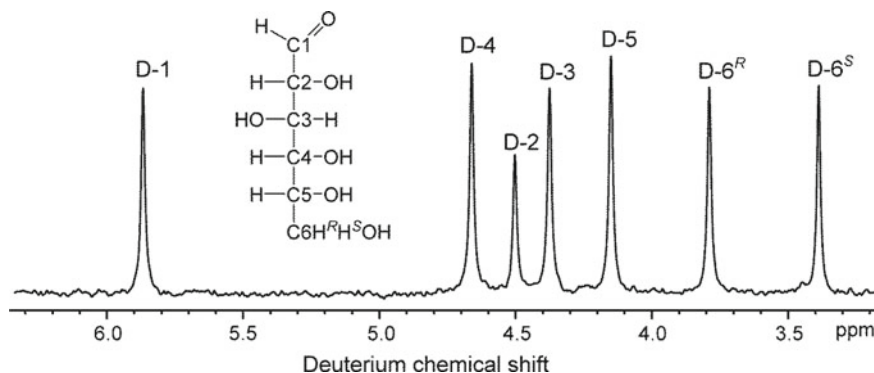
Fig. 7.5 ^{2}H NMR spectrum of a glucose derivative designed to give highly resolved spectra. The formula of glucose shows the assignment of the signals to isotopomers of glucose. Reproduced from Ehlers et al. (2015)

mass balance, or a reference molecule with known δ^2H is added to the NMR sample so that integrals in the ^{2}H spectrum can be linked to the δ^2H scale (Spahr et al. 2015).

7.4.1.2 Research Applications

As expected from the results on other metabolites, the intra-molecular ^{2}H distribution of tree-ring derived glucose is non-random (Betson et al. 2006). The intra-molecular variation is hundreds of ‰ large, much larger than for example the seasonal variation of δ^2H of precipitation. Because the intra-molecular variation influences δ^2H of the whole molecule, correlations of tree-ring δ^2H with climate variables are fraught with difficulty. Betson et al. (2006) also showed that the intra-molecular pattern of tree-ring cellulose is independent of the source water δ^2H. For metabolites on the leaf level, this can be expected, because when a metabolite is synthesized in a cellular compartment, all hydrogen that is incorporated into the molecule originates from the same water with a certain δ^2H. When tree-ring cellulose is synthesized, the ^{2}H isotopomer pattern may be modified by hydrogen exchange; that clear signals can be obtained from tree-ring cellulose may indicate that this exchange is constant over time. That the intramolecular pattern is independent of δ^2H means that signals that are based on isotopomer ratios can be extracted and interpreted without knowledge of δ^2H.

As mentioned above, intra-molecular isotope patterns reflect regulation of enzymes or metabolic pathways. Thus, they might respond to changes in metabolic fluxes. This was tested on glucose formed by plants using the C_3 photosynthetic pathway. In C_3 plants, the CO_2-fixing enzyme Rubisco can react with oxygen instead, in a side reaction that leads to C loss of the plant and which therefore is highly relevant for the global C cycle. Metabolites formed upon O_2 fixation are partly recycled to glucose in the so-called photorespiration cycle; therefore the isotopomer pattern of

C_3 glucose might reflect the ratio of O_2 to CO_2 fixation. As shown in Fig. 7.6a, the ^2H isotopomer pattern of C_3 glucose indeed depends on atmospheric CO_2 concentration during growth, expressed as function of $1/CO_2$ to reflect the $O_2:CO_2$ competition. The high correlation observed indicates that this isotopomer ratio is a clean measure
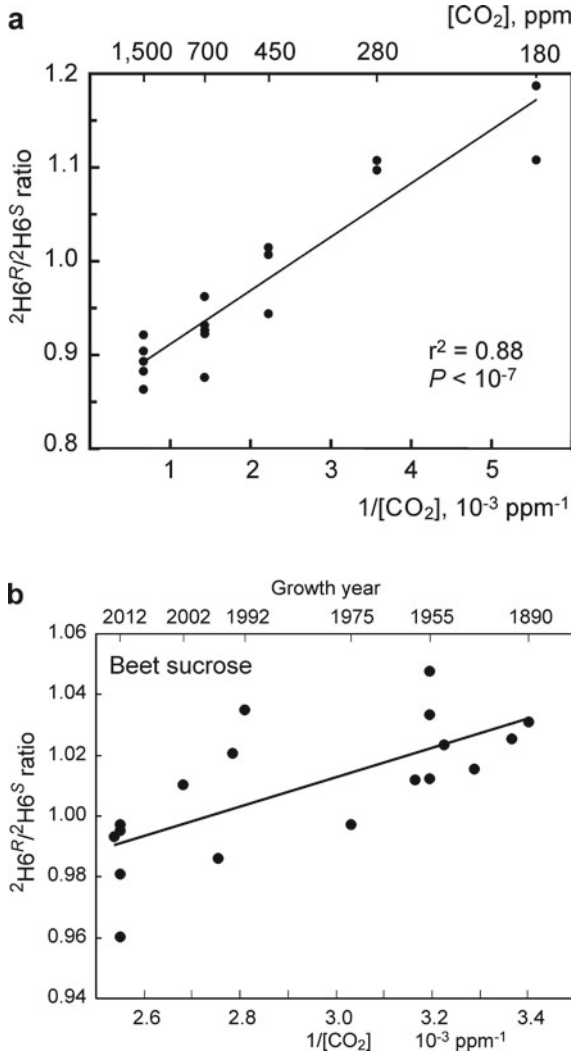

Fig. 7.6 Dependence of the ^2H-6^R/^2H-6^S isotopomer ratio (see Fig. 7.5) on $1/CO_2$ in **a** chamber-grown sunflowers ($r^2 = 0.88$, $P < 10^{-7}$, slope 0.057 ± 0.006 (SEM)) and **b** beet sugar samples formed between 1890 and 2012 ($r^2 = 0.49$, $P = 0.001$, slope $= 0.048 \pm 0.012$). The slopes of the isotopomer ratio as function of $1/CO_2$ are not significantly different. Reproduced from Ehlers et al. (2015)

of this metabolic flux ratio. This information cannot be achieved with δ^2H measurements on the whole molecule, because the dependence on the level of isotopomers gets averaged into the δ^2H of the whole molecule. The quantitative dependence of the ^2H isotopomer ratio on $1/CO_2$ was compared between plants grown in a CO_2 manipulation experiment and plants that grew at different times during the rise of atmospheric CO_2 concentration. Because there was no significant difference between the two data sets, it was concluded that increasing CO_2 concentration suppressed photorespiration to the same degree in the chamber studies and over the twentieth century. This also suggests that there was no acclimation response of plants over nearly a century, and demonstrates how long-term physiological information can be derived from isotopomers.

In contrast to the high correlations observed in Fig. 7.6, correlations of δ values with environmental parameters in tree-ring studies usually do not exceed $r^2 = 0.25$ (McCarroll and Loader 2004). We hypothesize that this is a general consequence of the averaging of isotopomer abundances into the δ value for the whole molecule of the respective isotope. The high correlations observed indicate that the ^2H-6^R/^2H-6^S ratio is determined by one metabolic process, namely the ratio of oxygenation to carboxylation, which is driven by atmospheric CO_2. Other isotopomer ratios may reflect other metabolic processes that may be driven by other environmental drivers (see below for ^{13}C). When a δ value is correlated with one environmental driver, it must be expected that isotopomer variation introduced by other environmental variables degrades this correlation, hence the curtailed correlation coefficients observed.

As glucose shows a non-random intra-molecular ^{13}C pattern (Gilbert et al. 2012; Gleixner and Schmidt 1997), the glucose units of tree-ring cellulose should also show a ^{13}C pattern. This expectation has been tested using a pine (*Pinus nigra*) tree-ring series (Wieloch et al. 2018). Figure 7.7 shows the observed ^{13}C isotopomer pattern. The ^{13}C variation of about $\pm 5‰$ is important for ^{13}C signals in the C cycle: When cellulose is decomposed in the environment, the $\delta^{13}C$ of the released CO_2 differs among the intra-molecular C positions. Thus, the $\delta^{13}C$ of respired CO_2 can vary, depending on whether the glucose units are completely respired to CO_2, or if the active metabolic pathway (such as fermentation) only releases some C positions as CO_2. Furthermore, it was observed that this ^{13}C pattern is variable over the tree-ring series (Wieloch et al. 2018). This variation must be caused by changes in environmental variables and hence it carries ecophysiological information. To analyse this, a hierarchical cluster analysis identified groups of ^{13}C isotopomers that vary independently of each other, which implies that they carry independent ecophysiological signals. One of these signals originates from the ^{13}C fractionation of diffusion and the ^{13}C isotope effect of Rubisco. The others are caused by yet unidentified ^{13}C fractionations downstream of Rubisco, and will hence carry new information. We hypothesize that isotopomer signals originating from such fractionations will shed light on processes such as C allocation. We anticipate that extracting such signals from tree-ring series can unravel acclimation responses of plants to environmental changes, a subject of great importance for the future of the biosphere as a C sink, and for crop productivity.
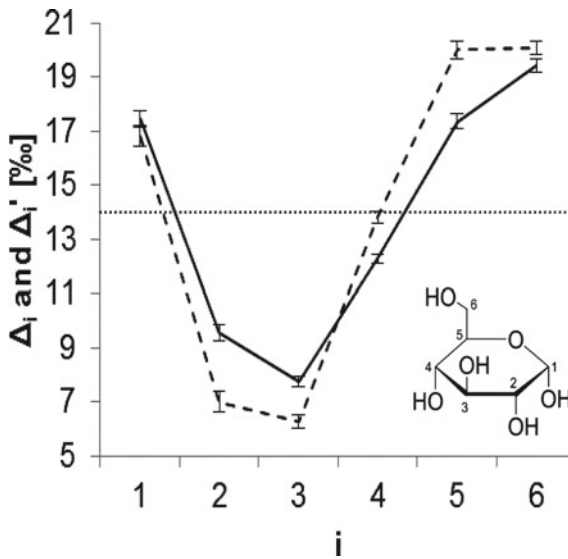
Fig. 7.7 ^{13}C isotopomer pattern of glucose units of tree-ring cellulose. The pattern connected by a solid line is the observed distribution, expressed as ^{13}C fractionation Δ_i for carbon i = 1–6; and the dashed line is a fractionation pattern $\Delta_i{}'$ that has been back-calculated to remove the isotope scrambling effect of triose phosphate cycling. Reproduced from Wieloch et al. (2018)

7.4.2 *Position-Specific $\delta^{18}O$*

Oxygen isotope ratios (δ^{18}O) in the annual growth rings of trees are considered to hold a valuable climatic and physiological records (Farquhar et al. 1998; Lehmann et al. 2017; McCarroll and Loader 2004; Sternberg et al. 2006) (see Chaps. 10, 16 and 19 for a more detailed discussion on climatic and physiological aspects of δ^{18}O). The original source of the oxygen atoms in tree-ring cellulose is soil moisture, generally obtained from precipitation, the δ^{18}O of which are closely linked to temperature (Chap. 18; Dansgaard 1964). Early hopes that δ^{18}O values of tree rings (e.g. Gray and Thompson 1976) could directly serve as a record for past temperature were overly optimistic. This is because the isotopic history of oxygen atoms from source water taken up by the tree and their final destination in trunk cellulose is complicated and, indeed, not fully understood (see Chap. 10 for more details). As a result of the processes involved, tree-ring cellulose is expected to carry a mixed soil water and leaf water signal in its oxygen atoms, complicating the process of abstracting climatic and physiological information from the oxygen isotope record (Roden et al. 2000). Position-specific isotope analysis of the oxygen atoms of cellulose holds out the hope of separating the leaf water and source water signals, especially if oxygen atoms at specific positions exchange either fully or not at all with stem water: the former group of oxygen atoms would be expected to provide a good record of source water, hence temperature, while the latter group would provide a good record of

leaf water, hence relative humidity. Progress in this field, however, has been much slower than is the case for position-specific carbon and hydrogen isotope analysis of cellulose (see Sect. 7.4.1). This is chiefly because, unlike ^{13}C and ^2H, ^{18}O does not have a nuclear spin and so does not produce an NMR signal. The lighter isotope (^{17}O) has a nuclear spin of 5/2; so that the ^{17}O nucleus has a quadrupole moment, which results in broad NMR peaks with poor resolution. This, combined with very low signal strengths resulting from the low natural abundance of ^{17}O (ca. 0.038%) means that ^{17}O NMR cannot at present be used to determine intra-molecular $\delta^{17}O$ values of samples with isotopes of natural abundance.

7.4.2.1 Sample Preparation and Analytical Methodology

To date, all methods published for the determination of $\delta^{18}O$ values at specific positions in the glucose rings of cellulose have involved a significant amount of synthetic organic chemistry in order to isolate or remove oxygen atoms from particular positions. Sternberg et al. (2003) reported the first of these methods, which was designed to determine the value of $\delta^{18}O$-2 of cellulose[1] by hydrolysing cellulose to glucose and then converting this to phenylglucosazone (Fig. 7.8a). Values of $\delta^{18}O$-2 were calculated from measured oxygen isotope ratios of cellulose ($\delta^{18}O_{cell}$) and phenyl-glucosazone ($\delta^{18}O_{PG}$) using an isotopic mass balance equation. The authors used cellulose from wheat seedlings (*Triticum aestivum*), which were grown in the dark in water samples differently enriched in ^{18}O, in order to simulate heterotrophic synthesis of cellulose in trunks of trees. The amount of cellulose required (1.5 g), however, is very high considering the amount of wood present in individual growth rings of trees. Results indicated that oxygen atoms at position 2 in cellulose completely exchanged with water, suggesting that $\delta^{18}O$-2 would be a better recorder of oxygen isotope ratios of soil water than is $\delta^{18}O_{cell}$. In a later study, however, Sternberg et al. (2006), using the same general synthetic method but with modified methods for hydrolysis of cellulose, obtained results indicating that only about 65–70% of the oxygen atoms at position 2 exchanged with water during cellulose synthesis. Importantly, the authors showed that there was no exchange between the oxygen atoms of cellulose and water during cellulose hydrolysis.

A different approach was made by Waterhouse et al. (2013), who described a method for the determination of the $\delta^{18}O$ value for each of the five oxygen positions in the glucose ring of cellulose. The overall process involved multiple synthetic steps, in which oxygen atoms from specific positions were removed and incorporated into molecules of benzoic acid (Fig. 7.8b). Benzoic acid samples were used for isotopic ratio measurement using GC/Pyr-IRMS. Reaction conditions had to be optimized to minimize the risk of isotopic fractionation during each step. As the authors acknowledge, a process with so many steps and the consequent need for large wood samples is unlikely to be practical for routine isotope analysis of tree-ring cellulose. The

---

[1] Oxygen atoms at specific positions in the cellulose molecule are designated 'O-n', where n is the same number as that of the carbon to which the oxygen atom is bonded—see Fig. 7.8a.
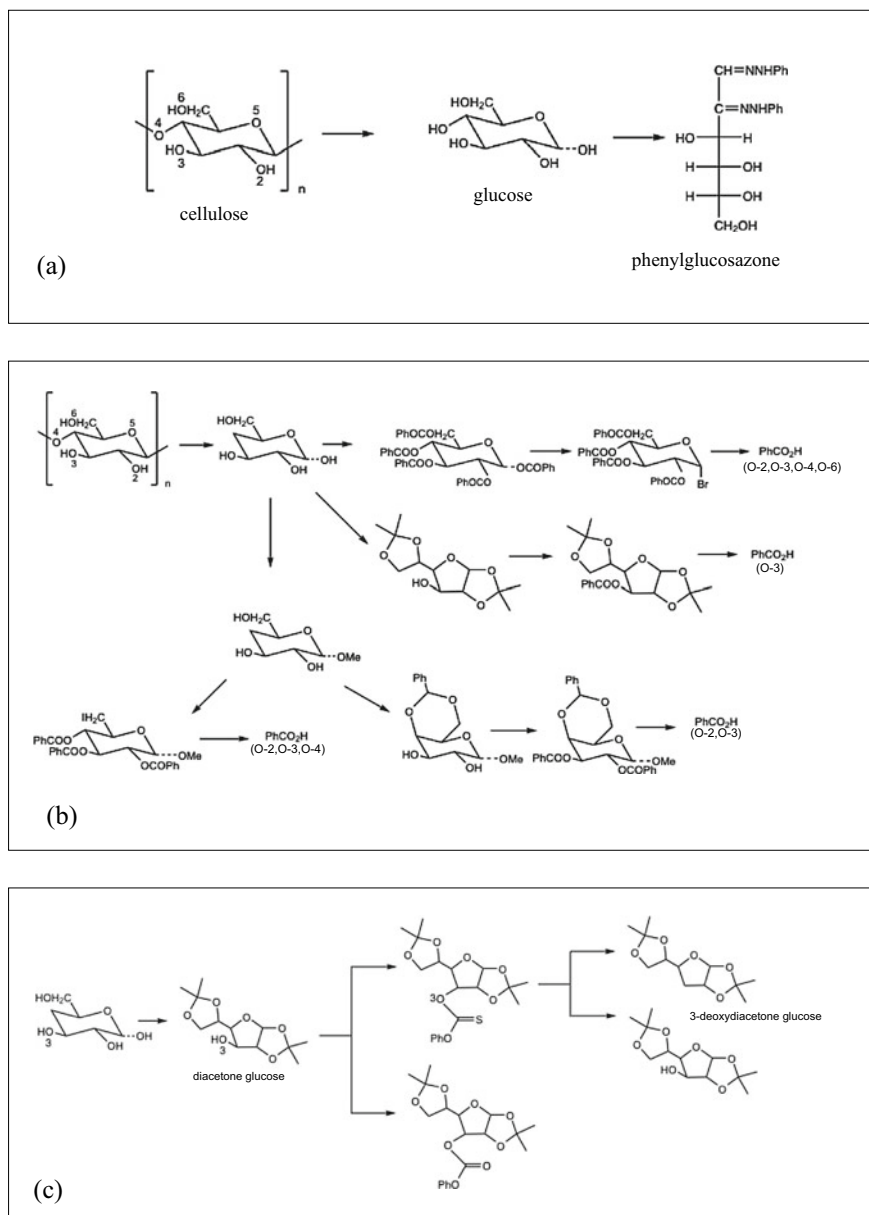
Fig. 7.8 Summaries of synthetic chemical steps involved in preparing samples for measuring oxygen isotope ratios at specific positions in cellulose. See cited literature for reagents and conditions. **a** Preparation of phenylglucosazone from cellulose (after Sternberg et al. 2003)—note numbering of oxygen atoms in the cellulose molecule. **b** Selective incorporation into benzoic acid (PhCO$_2$H) of oxygen atoms from indicated positions of cellulose (after Waterhouse et al. 2013). **c** Selective removal of O-3 from glucose by conversion of diacetone glucose to 3-deoxyacetone glucose (after Ma et al. 2018)

method was applied to α-cellulose samples obtained from wheat seedlings germinated in water of differing values of $\delta^{18}O$ (Sternberg et al. 2003), in order to determine the degree if isotopic exchange at each position during heterotrophic cellulose synthesis. Significant differences in the percentage exchange of oxygen with water at each position were detected: O-2 and O-4 showed little or no exchange; O-3, 48% exchange; O-5 and O-6, ca. 80% exchange. O-1, on the other hand, is derived from the water used in acid hydrolysis of cellulose. These results suggest that it is O-2 and O-4 that maintain chiefly a leaf water signal, whereas O-5 and O-6 should be the best targets for reconstructing source water isotope ratios. Significantly, the average of these percentage figures (41%) is close to the previously reported value (ca. 42%) for the percentage of oxygen exchange with trunk water during cellulose (Roden et al. 2000). The result that O-2 does not exchange is contrary to those of Sternberg et al. (2003) and Sternberg et al. (2006) but consistent with later results from samples from trees (Ellsworth et al. 2013; Sternberg et al. 2007)—see above; moreover, the enriched values of $\delta^{18}O$-2 (Ellsworth et al. 2013) are consistent with $\delta^{18}O$-2 of cellulose carrying a leaf-water signal enriched by evapotranspiration. However, oxygen at position 2 should have several opportunities to exchange with water during cellulose synthesis via reversible addition at carbonyl (Farquhar et al. 1998; Hill et al. 1995; Sternberg and DeNiro 1983); the fact that it seems not to exchange requires explanation.

More recently, a method for the determination of $\delta^{18}O$-3 of cellulose has been described (Ma et al. 2018). Like earlier methods, it comprises a sequence of synthetic steps and involves the same general strategy of Sternberg and colleagues described above: removal of the oxygen in question and calculation of its isotope ratio using an isotopic mass balance equation. In this case, glucose (from e.g. cellulose) is converted to diacetone glucose and O-3 removed by conversion to 3-deoxydiacetone glucose in a 2-step process (Fig. 7.8c). Values of $\delta^{18}O$-3 are calculated from $\delta^{18}O$ values of these two products measured using GC/Pyr-IRMS. One complication with the overall procedure is that the second and third synthetic steps each yield two products, allowing the possibility of a consequential change in the $\delta^{18}O$ value of 3-deoxydiacetone glucose. The authors calculate, however, that this is not significant. They also address the potential problem of error propagation, and show that overall the uncertainty in values of $\delta^{18}O$-3 could be as high as 1.3‰. Calculation of $\delta^{18}O$-3 of glucose derived from a C_4 plants suggested that this oxygen was isotopically enriched by around 12‰ relative to the average values of O-2 to O-6, confirming that there is isotopic inhomogeneity within the glucose molecule. Although the authors claim that their method would be suitable for a 50 mg sample of glucose, this still represents an inconveniently large amount of wood for routine application to samples from individual tree rings.

Despite the novelty of the above methods, they all require time-consuming synthetic procedures, which risk isotopic fractionation, and comparatively large amounts of material; there are also uncertainties regarding propagation of errors throughout the many procedures involved. Much still needs to be done before position-specific oxygen isotope analysis can be routinely applied to tree-ring samples.

7.4.2.2 Research Applications

There are only two reports in the literature on the application of position specific $\delta^{18}O$ analysis to tree samples, and both of them use the phenylglucosazone technique to obtain values of $\delta^{18}O$-2. In the first of these (Sternberg et al. 2007), trees were sampled from a wide range of latitudes across the northern hemisphere. Phenylglucosazone was prepared from glucose after acid hydrolysis of cellulose obtained from stem samples. Each sample of phenylglucosazone required comparatively large amounts (0.3 g) of wood. Comparison of values of $\delta^{18}O_{cell}$, $\delta^{18}O_{PG}$ and $\delta^{18}O$-2 (the latter was calculated from measured $\delta^{18}O_{cell}$, and $\delta^{18}O_{PG}$) with $\delta^{18}O_{sw}$ (measured from water removed from the stem) showed that $\delta^{18}O_{PG}$ was most closely related to $\delta^{18}O_{sw}$, whereas $\delta^{18}O$-2 was very poorly correlated with $\delta^{18}O_{sw}$. This result was unexpected, as O-2 had been previously reported to undergo exchange with source water to a high degree during heterotrophic cellulose synthesis (see above). The authors proposed that the lack of correlation resulted from 'isotopic noise' in values of $\delta^{18}O$-2 caused by the variety of species sampled and widely different values of $\delta^{18}O_{sw}$ across the wide geographical area of the study. One of the main conclusions was that phenyl-glucosazone presents a better record of $\delta^{18}O_{sw}$, and hence precipitation, than does cellulose itself.

In the second study (Ellsworth et al. 2013), phenylglucosazone was prepared from α-cellulose extracted from annual growth rings of trees growing in Finland, Switzerland and New Zealand. An innovation of the work was the modification of the synthesis of phenylglucosazone so that a smaller amount (25 mg) of cellulose could be used. This makes the technique more appropriate for the routine analysis of annual growth rings. As expected, removing O-2 from cellulose resulted in $^{18}O_{PG}$ having a much stronger relationship with $\delta^{18}O_{sw}$, hence higher potential for climatic reconstruction, than either $\delta^{18}O_{cell}$ or $\delta^{18}O$-2. Furthermore, the authors showed that values of $\delta^{18}O_{sw}$ calculated from measured $^{18}O_{PG}$ closely followed observed values of $\delta^{18}O_{sw}$ in both magnitude and temporal variability, whereas values of $\delta^{18}O_{sw}$ calculated from $\delta^{18}O$-2 were both significantly enriched and much more variable than observed values.

References

Barbour MM, Song X (2014) Do tree-ring stable isotope compositions faithfully record tree carbon/water dynamics? Tree Physiol 34:792–795

Barrie A, Bricout J, Koziet J (1984) Gas chromatography—stable isotope ratio analysis at natural abundance levels. Biomed Mass Spectrom 11:583

Battibaglia G, De Micco V, Brand WA, Linke P, Aronne G, Saurer M, Cherubini P (2010) Variations of vessel diameter and $\delta^{13}C$ in false rings of *Arbutus unedo* L. reflect different environmental conditions. New Phytol 188:1099–1112

Betson TR, Augusti A, Schleucher J (2006) Quantification of deuterium isotopomers of tree-ring cellulose using nuclear magnetic resonance. Anal Chem 78:8406–8411

Blees J, Saurer M, Siegwolf R, Ulevicius V, Prevôt A, Dommen J, Lehmann M (2017) Oxygen isotope analysis of levoglucosan, a tracer of wood burning, in experimental and ambient aerosol samples. Rapid Commun Mass Spectrom 31:2101–2108

Blokhina O, Valerio C, Sokolowska K, Zhao L, Karkonen A, Niittyla T, Fagerstedt K (2017) Laser capture microdissection protocol for xylem tissues of woody plants. Front Plant Sci 7

Bogelein R, Lehmann MM, Thomas FM (2019) Differences in carbon isotope leaf-to-phloem fractionation and mixing patterns along a vertical gradient in mature European beech and Douglas fir. New Phytol 222:1803–1815

Boschker HT, Moerdijk-Poortvliet TC, van Breugel P, Houtekamer M, Middelburg JJ (2008) A versatile method for stable carbon isotope analysis of carbohydrates by high-performance liquid chromatography/isotope ratio mass spectrometry. Rapid Commun Mass Spectrom 22:3902–3908

Brandes E, Kodama N, Whittaker K, Weston C, Rennenberg H, Keitel C, Adams MA, Gessler A (2006) Short-term variation in the isotopic composition of organic matter allocated from the leaves to the stem of *Pinus sylvestris*: effects of photosynthetic and postphotosynthetic carbon isotope fractionation. Glob Chang Biol 12:1922–1939

Bruykhanova MV, Vaganov EA, Wirth C (2011) Influence of climatic factors and reserve assimilates on the radial growth and carbon isotope composition in tree rings of deciduous and coniferous species. Contemp Probl Ecol 4:126–132

Cernusak LA, Wong SC, Farquhar GD (2003) Oxygen isotope composition of phloem sap in relation to leaf water in *Ricinus communis*. Funct Plant Biol 30:1059–1070

Cernusak LA, Farquhar GD, Pate JS (2005) Environmental and physiological controls over oxygen and carbon isotope composition of Tasmanian blue gum, *Eucalyptus globulus*. Tree Physiol 25:129–146

Cernusak LA, Tcherkez G, Keitel C, Cornwell WK, Santiago LS, Knohl A, Barbour MM, Williams DG, Reich PB, Ellsworth DS, Dawson TE, Griffiths HG, Farquhar GD, Wright IJ (2009) Why are non-photosynthetic tissues generally 13C enriched compared with leaves in C3 plants? Review and synthesis of current hypotheses. Funct Plant Biol 36:199

Cernusak LA, Barbour MM, Arndt SK, Cheesman AW, English NB, Feild TS, Helliker BR, Holloway-Phillips MM, Holtum JAM, Kahmen A, McInerney FA, Munksgaard NC, Simonin KA, Song X, Stuart-Williams H, West JB, Farquhar GD (2016) Stable isotopes in leaf water of terrestrial plants. Plant Cell Environ 39:1087–1102

Chaintreau A, Fieber W, Sommer H, Gilbert A, Yamada K, Yoshida N, Pagelot A, Moskau D, Moreno A, Schleucher J, Reniero F, Holland M, Guillou C, Silvestre V, Akoka S, Remaud GS (2013) Site-specific 13C content by quantitative isotopic 13C nuclear magnetic resonance spectrometry: a pilot inter-laboratory study. Anal Chim Acta 788:108–113

Churakova (Sidorova) O, Lehmann M, Saurer M, Fonti M, Siegwolf R, Bigler C (2018) Compound-specific carbon isotopes and concentrations of carbohydrates and organic acids as indicators of tree decline in Mountain pine. Forests 9:363

Churakova (Sidorova) OV, Lehmann MM, Siegwolf RTW, Saurer M, Fonti MV, Schmid L, Timofeeva G, Rinne-Garmston KT, Bigler C (2019) Compound-specific carbon isotope patterns in needles of conifer tree species from the Swiss National Park under recent climate change. Plant Physiol Biochem 139:264–272

Cuny HE, Rathgeber CBK, Senga Kiessé T, Hartmann FP, Barbeito I, Fournier M (2013) Generalized additive models reveal the intrinsic complexity of wood formation dynamics. J Exp Bot 64:1983–1994

Dansgaard W (1964) Stable isotopes in precipitation. Tellus 16:436–468

De Niro MJ, Epstein S (1977) Mechanisms of carbon isotope fractionation associated with lipid-synthesis. Science 197:261–263

De Micco V, Battibaglia G, Brand WA, Linke P, Saurer M, Aronne G, Cherubini P (2012) Discrete versus continuous analysis of anatomical and $\delta^{13}C$ variability in tree rings with intra-annual density fluctuations. Trees 26:513–524

Dennis DT, Blakeley SD (2000) Carbohydrate metabolism. In: Biochemistry and molecular biology of plants. American Society of Plant Physiologists, Rockville MD, USA

Ehlers I, Augusti A, Betson TR, Nilsson MB, Marshall JD, Schleucher J (2015) Detecting long-term metabolic shifts using isotopomers: CO_2-driven suppression of photorespiration in C3 plants over the 20th century. Proc Natl Acad Sci 112:15585–15590

Ellsworth PV, Anderson WT, Sonninen E, Barbour MM, Sternberg LSL (2013) Reconstruction of source water using the $\delta^{18}O$ of tree ring phenylglucosazone: a potential tool in paleoclimate studies. Dendrochronologia 31:153–158

Farquhar GD, O'Leady MH, Berry JA (1982) On the relationship between carbon isotope discrimination and the intercellular carbon dioxide concentration in leaves. Aust J Plant Physiol 9:121–137

Farquhar GD, Barbour MM, Henry BK (1998) Interpretation of oxygen isotope composition of leaf material. In: Stable isotopes: the integration of biological, ecological and geochemical processes. BIOS Scientific, Oxford, pp 27–62

Fonti MV, Vaganov EA, Wirth C, Shashkin AV, Astrakhantseva NV, Schulze ED (2018) Age-effect on intra-annual $\delta^{13}C$-variability within Scots pine tree-rings from central Siberia. Forests 9:1–14

Ford CW (1984) Accumulation of low molecular weight solutes in waterstressed tropical legumes. Phytochemistry 23:1007–1015

Forster T, Schweingruber FH, Denneler B (2000) Increment puncher: a tool for extracting small cores of wood and bark from living trees. IAWA J 21:169–180

Galiano L, Timofeeva G, Saurer M, Siegwolf R, Martinez-Vilalta J, Hommel R, Gessler A (2017) The fate of recently fixed carbon after drought release: towards unravelling C storage regulation in *Tilia platyphyllos* and *Pinus sylvestris*. Plant Cell Environ 40:1711–1724

Gessler A, Brandes E, Keitel C, Boda S, Kayler ZE, Granier A, Barbour M, Farquhar GD, Treydte K (2013) The oxygen isotope enrichment of leaf-exported assimilates—does it always reflect lamina leaf water enrichment? New Phytologist 200:144–157

Gessler A, Rennenberg H, Keitel C (2004) Stable isotope composition of organic compounds transported in the phloem of European beech—evaluation of different methods of phloem sap collection and assessment of gradients in carbon isotope composition during leaf-to-stem transport. Plant Biol 6:721–729

Gessler A, Tcherkez G, Karyanto O, Keitel C, Ferrio JP, Ghashghaie J, Kreuzwieser J, Farquhar GD (2009) On the metabolic origin of the carbon isotope composition of CO_2 evolved from darkened light-acclimated leaves in *Ricinus communis*. New Phytol 181:374–386

Gessler A, Ferrio JP, Hommel R, Treydte K, Werner RA, Monson RK (2014) Stable isotopes in tree rings: towards a mechanistic understanding of isotope fractionation and mixing processes from the leaves to the wood. Tree Physiol 34:796–818

Gilbert A, Silvestre V, Robins RJ, Tcherkez G, Remaud GS (2011) A ^{13}C NMR spectrometric method for the determination of intramolecular delta^{13}C values in fructose from plant sucrose samples. New Phytol 191:579–588

Gilbert A, Silvestre V, Robins RJ, Remaud GS, Tcherkez G (2012) Biochemical and physiological determinants of intramolecular isotope patterns in sucrose from C-3, C-4 and CAM plants accessed by isotopic ^{13}C NMR spectrometry: a viewpoint. Nat Prod Rep 29:476–486

Gleixner G, Schmidt H-L (1997) Carbon isotope effects on the fructose-1,6-bisphosphate aldolase reaction, origin for non-statistical ^{13}C distributions in carbohydrates. J Biol Chem 272:5382–5387

Gleixner G, Danier H-J, Werner RA, Schmidt H-L (1993) Correlations between the ^{13}C content of primary and secondary plant products in different cell compartments and that in decomposing basidiomycetes. Plant Physiol 102:287–1290

Gleixner G, Scrimgeour C, Schmidt H-L, Viola R (1998) Stable isotope distribution in the major metabolites of source and sink organs of *Solanum tuberosum* L.: a powerful tool in the study of metabolic partitioning in intact plants. Planta 207:241–245

Gray J, Thompson P (1976) Climatic information from $^{18}O/^{16}O$ ratios of cellulose in tree-rings. Nature 262:481–482

Helle G, Schleser GH (2004) Beyond CO_2-fixation by Rubisco—an interpretation of $^{13}C/^{12}C$ variations in tree rings from novel intra-seasonal studies on broad-leaf trees. Plant Cell Environ 27:367–380

Helliker BR, Ehleringer JR (2002) Differential ^{18}O enrichment of leaf cellulose in C_3 versus C_4 grasses. Funct Plant Biol 29:435–442

Hepp J, Rabus M, Anhauser T, Bromm T, Laforsch C, Sirocko F, Glaser B, Zech M (2016) A sugar biomarker proxy for assessing terrestrial versus aquatic sedimentary input. Org Geochem 98:98–104

Hill SA, Waterhouse JS, Field EM, Switsur VR, Ap Rees T (1995) Rapid recycling of triose phosphates in oak stem tissue. Plant Cell Environ 18:931–936

Hobbie EA, Werner RA (2004) Intramolecular, compound-specific, and bulk carbon isotope patterns in C_3 and C_4 plants: a review and synthesis. New Phytol 161:371–385

Kagawa A, Naito D, Sugimoto A, Maximov TC (2003) Effects of spatial and temporal variability in soil moisture on widths and $\delta^{13}C$ values of eastern Siberian tree rings. J Geophys Res 108

Kornexl BE, Werner RA, Gehre M (1999) Standardization for oxygen isotope ratio measurement—still an unsolved problem. Rapid Commun Mass Spectrom 13:1248–1251

Kornexl BE, Gehre M, Hofling R, Werner RA (1999) On-line $\delta^{18}O$ measurement of organic and inorganic substances. Rapid Commun Mass Spectrom 13:1685–1693

Krummen M, Hilkert AW, Juchelka D, Duhr A, Schluter HJ, Pesch R (2004) A new concept for isotope ratio monitoring liquid chromatography/mass spectrometry. Rapid Commun Mass Spectrom 18:2260–2266

Kuroda K, Fujiwara T, Hashida K, Imai T, Kushi M, Saito K, Fukushima K (2014) The accumulation pattern of ferruginol in the heartwood-forming *Cryptomeria japonica* xylem as determined by time-of-flight secondary ion mass spectrometry and quantity analysis. Ann Bot 113:1029–1036

Lehmann MM, Rinne KT, Blessing C, Siegwolf RT, Buchmann N, Werner RA (2015) Malate as a key carbon source of leaf dark-respired CO_2 across different environmental conditions in potato plants. J Exp Bot 66:5769–5781

Lehmann MM, Fischer M, Blees J, Zech M, Siegwolf RT, Saurer M (2016) A novel methylation derivatization method for $\delta^{18}O$ analysis of individual carbohydrates by gas chromatography/pyrolysis-isotope ratio mass spectrometry. Rapid Commun Mass Spectrom 30:221–229

Lehmann MM, Gamarra B, Kahmen A, Siegwolf RTW, Saurer M (2017) Oxygen isotope fractionations across individual leaf carbohydrates in grass and tree species. Plant Cell Environ 40:1658–1670

Lehmann MM, Goldsmith GR, Schmid L, Gessler A, Saurer M, Siegwolf RTW (2018) The effect of (18) O-labelled water vapour on the oxygen isotope ratio of water and assimilates in plants at high humidity. New Phytol 217:105–116

Lehmann MM, Egli M, Brinkmann N, Werner RA, Saurer M, Kahmen A (2020). Improving the extraction and purification of leaf and phloem sugars for oxygen isotope analyses. Rapid Communications in Mass Spectrometry 34 (19):8854

Lehmann MM, Goldsmith GR, Mirande-Ney C, Weigt RB, Schönbeck L, Kahmen A, Gessler A, Siegwolf RTW, Saurer M (2019) The ^{18}O-signal transfer from water vapour to leaf water and assimilates varies among plant species and growth forms. Plant Cell Environ

Lipavská H, Svobodová H, Albrechtová J (2000) Annual dynamics of the content of non-structural saccharides in the context of structural development of vegetative buds of Norway spruce. J Plant Physiol 157:365–373

Loader NJ, Robertson I, Barker AC, Switsur VR, Waterhouse JS (1997) An improved method for the batch processing of small whole wood samples to α-cellulose. Chem Geol 136:313–317

Loader NJ, McCarroll D, Barker S, Jalkanen R, Grudd H (2017) Inter-annual carbon isotope analysis of tree-rings by laser ablation. Chem Geol 466:323–326

Long A, Arnold LD, Larry D, Damon PE, Lerman JC, Wilson AT (1979) Radial translocation of carbon in bristlecone pine. Proceedings ninth international conference on radiocarbon dating, Los Angeles and La Jolla. Berkeley, University of California Press, pp 532–537

Ma R, Zhu Z, Wang B, Zhoa Y, Yin X, Lu F, Wang Y-P, Su J, Hocart CH, Zhou Y (2018) Novel position-specific $^{18}O/^{16}O$ Measurement of carbohydrates. I. O-3 of glucose and confirmation of $^{18}O/^{16}O$ heterogeneity at natural abundance levels inn glucose from starch of C_4 plants. Anal Chem 90:10293–10301

Macko SA, Ryan M, Engel M (1998) Stable isotopis analysis of individual carbohydrates by GC/C/IRMS. Chem Geol 152:205–210

Martin GJ, Martin ML, Zhang BL (1992) Site-specific natural isotope fractionation of hydrogen in plant products studied by nuclear magnetic resonance. Plant Cell Environ 15:1037–1050

Mauve C, Bleton J, Bathellier C, Lelarge-Trouverie C, Guerard F, Ghashghaie J, Tchapla A, Tcherkez G (2009) Kinetic $^{12}C/^{13}C$ isotope fractionation by invertase: evidence for a small in vitro isotope effect and comparison of two techniques for the isotopic analysis of carbohydrates. Rapid Commun Mass Spectrom 23:2499–2506

McCarroll D, Loader NJ (2004) Stable isotopes in tree rings. Quat Sci Rev 23:771–801

Míková J, Košler J, Widenbeck M (2014) Matrix effects during laser ablation MC ICP-MS analysis of boron isotopes in tourmaline. J Anal At Spectrom 29:903–914

Moing A (2000) Sugar alcohols as carbohydrate reserves in some higher plants. In: Carbohydrate reserves in plant—synthesis and regulation. Elsevier Science BV, Amsterdam, The Netherlands

Morrison DJ, Taylor K, Preston T (2010) Strong anion-exchange liquid chromatography coupled with isotope ratio mass spectrometry using a Liquiface interface. Rapid Commun Mass Spectrom 24:1755–1762

Panek JA, Waring RH (1997) Stable carbon isotopes asa indicators of limitations to forest growth imposed by climate stress. Ecol Appl 7:854–863

Rinne KT, Boettger T, Loader NJ, Robertson I, Switsur VR, Waterhouse JS (2005) On the purification of α-cellulose from resinous wood for stable isotope (H, C and O) analysis. Chem Geol 222:75–82

Rinne KT, Saurer M, Streit K, Siegwolf RT (2012) Evaluation of a liquid chromatography method for compound-specific delta^{13}C analysis of plant carbohydrates in alkaline media. Rapid Commun Mass Spectrom 26:2173–2185

Rinne KT, Saurer M, Kirdyanov AV, Loader NJ, Bryukhanova MV, Werner RA, Siegwolf RT (2015) The relationship between needle sugar carbon isotope ratios and tree rings of larch in Siberia. Tree Physiol 35:1192–1205

Rinne KT, Saurer M, Kirdyanov AV, Bryukhanova MV, Prokushkin AS, Churakova (Sidorova) OV, Siegwolf RTW (2015a) Examining the response of needle carbohydrates from Siberian larch trees to climate using compound-specific δ^{13}C and concentration analyses. Plant Cell Environ 38:2340–2352

Roden JS, Lin G, Ehleringer JR (2000) A mechanistic model for interpretation of hydrogen and oxygen isotope ratios in tree-ring cellulose. Geochim Cosmochim Acta 64:21–35

Romek KM, Krzeminska A, Remaud GS, Julien M, Paneth P, Robins RJ (2017) Insights into the role of methionine synthase in the universal C-13 depletion in O- and N-methyl groups of natural products. Arch Biochem Biophys 635:60–65

Rossi S, Anfodillo T, Menardi R (2006) Trephor: a new tool for sampling microcores from tree stems. IAWA J 27:89–97

Rossmann A, Butzenlechner M, Schmidt HL (1991) Evidence for a nonstatistical carbon isotope distribution in natural glucose. Plant Physiol 96:609–614

Scheidegger Y, Saurer M, Bahn M, Siegwolf R (2000) Linking stable oxygen and carbon isotopes with stomatal conductance and photosynthetic capacity: a conceptual model. Oecologia 125:350–357

Schmidt HL (2003) Fundamentals and systematics of the non-statistical distributions of isotopes in natural compounds. Naturwissenschaften 90:537–552

Schollaen K, Heinrich I, Helle G (2014) UV-laser-based microscopic dissection of tree rings—a novel sampling tool for delta(13) C and delta(18) O studies. New Phytol 201:1045–1055

Schollaen K, Baschek H, Heinrich I, Slotta F, Pauly M, Helle G (2017) A guideline for sample preparation in modern tree-ring stable isotope research. Dendrochronologia 44:133–145

Schulze B, Wirth C, Linke P, Brand WA, Kuhlmann I, Horna V, Schulze ED (2004) Laser ablation-combustion-GC-IRMS—a new method for online analysis of intra-annual variation of δ^{13}C in tree rings. Tree Physiol 24:1193–1201

Schweingruber FH, Börner A, Schulze E-D (2006) Atlas of woody plant stems: evolution, structure, and environmental modifications. Springer, Berlin

Skomarkova MV, Vaganov EA, Mund M, Knohl A, Linke P, Boerner A, Schulze ED (2006) Inter-annual and seasonal variability of radial growth, wood density and carbon isotope ratios in tree rings of beech (Fagus sylvatica) growing in Germany and Italy. Trees 20:571–586

Smith M, Wild B, Richter A, Simonin K, Merchant A (2016) Carbon isotope composition of carbohydrates and polyols in leaf and phloem sap of Phaseolus vulgaris L. influences predictions of plant water use efficiency. Plant Cell Physiol 57:1756–1766

Soudant A, Loader NJ, Bäck J, Levula J, Kljun N (2016) Intra-annual variability of wood formation and δ^{13}C in tree-rings at Hyytiälä, Finland. Agric For Meteorol 224:17–29

Spahr S, Bolotin J, Schleucher J, Ehlers I, von Gunten U, Hofstetter TB (2015) Compound-specific carbon, nitrogen, and hydrogen isotope analysis of N-nitrosodimethylamine in aqueous solutions. Anal Chem 87:2916–2924

Sternberg LSL, DeNiro MJ (1983) Biogeochemical implications of the isotopic equilibrium fractionation factor between the oxygen atoms of acetone and water. Geochim Cosmochim Acta 47:2271–2274

Sternberg LSL, Anderson WT, Morrison K (2003) Separating soil and leaf water ^{18}O isotopic signals in plant stem cellulose. Geochim Cosmochim Acta 67:2561–2566

Sternberg LSL, Pinzon MC, Anderson WT, Jahren AH (2006) Variation in oxygen isotope fractionation during cellulose synthesis: intramolecular and biosynthetic effects. Plant Cell Environ 29:1881–1889

Sternberg LSL, Pinzon MC, Vendramini PF, Anderson WT, Jahren AH, Beuning K (2007) Oxygen isotope ratios of cellulose-derived phenylglucosazone: an improved paleoclimate indicator of environmental water and relative humidity. Geochim Cosmochim Acta 71:2463–2473

Streit K, Rinne KT, Hagedorn F, Dawes MA, Saurer M, Hoch G, Werner RA, Buchmann N, Siegwolf RT (2013) Tracing fresh assimilates through Larix decidua exposed to elevated CO(2) and soil warming at the alpine treeline using compound-specific stable isotope analysis. New Phytol 197:838–849

Treydte K, Boda S, Graf Pannatier E, Fonti P, Frank D, Ullrich B, Saurer M, Siegwolf R, Battipaglia G, Werner W, Gessler A (2014) Seasonal transfer of oxygen isotopes from precipitation and soil to the tree ring: source water versus needle water enrichment. New Phytol 202:772–783

Treydte K, Frank D, Esper J, Andreu L, Bednarz Z, Berninger F, Boettger T, D'Alessandro CM, Etien N, Filot M, Grabner M, Guillemin MT, Gutierrez E, Haupt M, Helle G, Hilasvuori E, Jungner H, Kalela-Brundin M, Krapiec M, Leuenberger M, Loader NJ, Masson-Delmotte V, Pazdur A, Pawelczyk S, Pierre M, Planells O, Pukiene R, Reynolds-Henne CE, Rinne KT, Saracino A, Saurer M, Sonninen E, Stievenard M, Switsur VR, Szczepanek M, Szychowska-Krapiec E, Todaro L, Waterhouse JS, Weigl M, Schleser GH (2007) Signal strength and climate calibration of a European tree-ring isotope network. Geophys Res Lett 34

Vaganov EA, Schulze ED, Skomarkova MV, Knohl A, Brand WA, Roscher C (2009) Intra-annual variability of anatomical structure and delta(13)C values within tree rings of spruce and pine in alpine, temperate and boreal Europe. Oecologia 161:729–745

Vysotskaya LG, Shashkin AV, Vaganov EA (1985) Analysis of the size distribution of tracheids in the annual rings of pines growing under various moisture conditions. Sov J Ecol 16:29–34

Walcroft AS, Silvester WB, Whitehead D, Kelliher FM (1997) Seasonal changes in stable carbon isotope ratios within annual rings of *Pinus radiata* reflect environmental regulation of growth processes. Aust J Plant Physiol 24:57–68

Wanek W, Heintel S, Richter A (2001) Preparation of starch and other carbon fractions from higher plant leaves for stable carbon isotope analysis. Rapid Commun Mass Spectrom 15:1136–1140

Waterhouse JS, Cheng S, Juchelka D, Loader NJ, McCarroll D, Switsur VR, Gautam L (2013) Position-specific measurement of oxygen isotope ratios in cellulose: isotopic exchange during heterotrophic cellulose synthesis. Geochim Cosmochim Acta 112:178–191

Weigt RB, Braunlich S, Zimmermann L, Saurer M, Grams TE, Dietrich HP, Siegwolf RT, Nikolova PS (2015) Comparison of delta(18)O and delta(13)C values between tree-ring whole wood and cellulose in five species growing under two different site conditions. Rapid Commun Mass Spectrom 29:2233–2244

West AG, Patrickson SJ, Ehleringer JR (2006) Water extraction times for plant and soil materials used in stable isotope analysis. Rapid Commun Mass Spectrom 20:1317–1321

Wieloch T, Ehlers I, Yu J, Frank D, Grabner M, Gessler A, Schleucher J (2018) Intramolecular (13)C analysis of tree rings provides multiple plant ecophysiology signals covering decades. Sci Rep 8:5048

Wild B, Wanek W, Postl W, Richter A (2010) Contribution of carbon fixed by Rubisco and PEPC to phloem export in the Crassulacean acid metabolism plant Kalanchoe daigremontiana. J Exp Bot 61:1375–1383

Williams JHH, Collis BE, Pollock CJ, Williams ML, Farrar JF (1993) Variability in the distribution of photoassimilates along leaves of temperate Gramineae. New Phytol 123:699–703

Zech M, Glaser B (2009) Compound-specific $\delta^{18}O$ analyses of neutral sugars in soils using gas chromatography-pyrolysis-isotope ratio mass spectrometry: problems, possible solutions and a first application. Rapid Commun Mass Spectrom 23:3522–3532

Zech M, Saurer M, Tuthorn M, Rinne KT, Werner RA, Siegwolf R, Glaser B, Juchelka D (2013) A novel methodological approach for $\delta^{18}O$ analysis of sugars using gas chromatography-pyrolysis-isotope ratio mass spectrometry. Isot Environ Health Stud 49:492–502

Zech M, Tuthorn M, Detsch F, Rozanski K, Zech R, Zoller L, Zech W, Glaser B (2013) A 220 ka terrestrial $\delta^{18}O$ and deuterium excess biomarker record from an eolian permafrost paleosol sequence, NE-Siberia. Chem Geol 360:220–230